2009

The Effect of Adsorbent Geometry and Surface Chemistry on HPLC Retention

Zhaoxia Liu
Seton Hall University

The Effect of Adsorbent Geometry and Surface

Chemistry on HPLC retention

By:

Zhaoxia Liu

Dissertation submitted to the

Department of Chemistry & Biochemistry of

Seton Hall University

In partial fulfillment of the requirements for the degree of
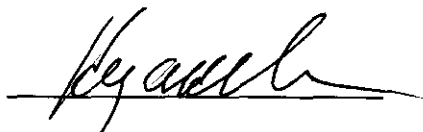
DOCTOR OF PHILOSOPHY

In

Chemistry

May, 2009

South Orange, New Jersey
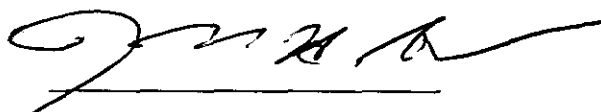
We certify that we have read this dissertation and that, in our opinion, it is adequate in scientific scope and quality as a dissertation for the degree of Doctor of Philosophy.

Approved

Yuri V. Kazakevich, Ph. D.

Research Mentor

Nicholas H. Snow, Ph.D.

Member of Dissertation Committee

Alexander Fadeev, Ph.D.

Member of Dissertation Committee

Nicholas H. Snow, Ph.D.

Chair, Department of Chemistry and Biochemistry

Table of contents

List of Figures

List of Tables

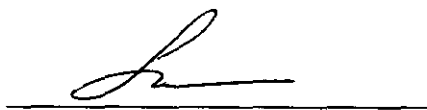# The effect of Adsorbent Geometry and Surface Chemistry on HPLC retention

Abstract

Recent development of new HPLC packing materials calls for extended studies of the influence of adsorbent geometry on analyte retention. Porosity and accessible surface area affect column selectivity and overall retention. Analyte transport inside the adsorbent porous space could be interpreted as superposition of active (pressure driven) and diffusive flow. Adsorbent surface chemistry and energetic heterogeneity are also important factors affecting analyte retention. Chemical modification of the adsorbent alters not only the surface chemistry but also geometry of porous material. The individual influence of each of these parameters is the key for targeted synthesis of HPLC packing material.

Six reversed-phase columns from different manufacturers were characterized in terms of adsorbent geometry (e.g., pore volume, surface area, column void volume, and inter-particle volume). Measurement of the surface area of chemically modified silica-based adsorbents is discussed together with the methods for the determination of the amount of adsorbent in the column. The behavior of nearly ideal chromatographic systems was studied. Retention factors of alkylbenzenes in MeCN/H_2O and MeOH/H_2O systems were compared with surface specific retention factors. The distribution of conventional retention factor values for the same analyte among the six columns using identical chromatographic conditions exceeded 35%, while the relative standard deviation of surface-specific retention factors was on the level of 3%.

x

The surface excess adsorption isotherms of the organic eluent components (MeCN and MeOH) from H_2O were measured on the porous silica surface from six reversed-phase columns. The study of the modified surface area provides a better evaluation of the excess adsorption behaviors of the stationary phases. The adsorption isotherms can give useful information about the surface heterogeneity of the stationary phase. Based on that the adsorption isotherm becomes negative when the composition is close to 100% (v/v) of organic modifier, the unreacted silanol groups on the bonded phase preferentially adsorb H_2O in the mobile phase. The hydrophilic mole fractions on the surface were compared with the excess adsorption isotherm. Allure-C_{18} shows the least negative excess and has the lowest value of hydrophilic mole fraction, which agrees to the highest value of bonding density.

This work is dedicated to my family:

My mother:

Manrong Wu

My daughter:

Angela Zhao

And it is in memory of

My father:

Xingwei Liu

Acknowledgements

I would like to extend my gratitude to Dr. Yuri Kazakevich, for his guidance, patience, encouragement and fruitful discussions. He led me to the exciting chromatography field. What I learned from him is very beneficial to both school and work. His open mindedness and encouragement to pursue the answers in my reserach projects enhanced my enjoyment. His remarkable enthusiasm and high standards for scientific research will positively influence my future career.

I would also like to thank Dr. Nicholas Snow and Dr. Alexander Fadeev for reviewing my thesis, and thank the committee members, for the time and assistance in my graduate study. I want to thank Mrs. Helen Kubowicz and Dr. Yufeng Wei for their help with the paperwork for my graduation. I also value the assistance given to me by the faculty and students in the Department of Chemistry. It is difficult to name all the people who have helped make this program's completion possible.

I am thankful to the Separation Science group at Seton Hall University for the interesting discussions, with special thanks addressed to Mr. Alex Yeung, Mr. Alex Giaquinto, and Mr. Andrew Bach.

On the non-academic side, I am grateful to Novartis Pharmaceutical Corporation for providing financial support. Special thanks to Mr. Patrick Drumm and Dr. Richard Thompson for their strong support. I would also like to thank Mr. Eric Loeser for helpful discussion and valuable suggestion in my writing. Thanks very much to Mr. Stanislaw Babiak for the motivation and strong support.

Finally, many thanks go to my family and friends for their ceaseless support, especially my mom, Manrong Wu and my daughter, Angela Zhao.

Dissertation Structure

The research described within this thesis is composed of a description of new interpretation of HPLC retention and studies of surface heterogeneity from adsorption of organic eluent components on different types of silica.

HPLC retention is based on the retention factor, which in turn is associated with the stationary phase volume or adsorbent surface area. In both case, proper characterization of packing materials geometry is necessary. Association of chromatographic retention with available adsorbent surface should allow for better correlation between different reversed-phase columns. In this work we discuss the problems associated with the evaluation of the actual geometry parameters of different commercial columns and compare the surface corrected retention data for these columns, and study the surface heterogeneity based on the eluent adsorption behaviors on the surfaces of commercially available C_{18} columns

Section 1 shows the background and history of different approaches undertaken to study the retention behavior and characterization of bonded silica in RPLC. Proper characterization of geometric parameters, especially the surface area, is essential in determining eluent components adsorption and the comparison of chromatographic behaviors. The eluent component adsorption behavior on reversed-phase bonded ligands is discussed. Interpretation of excess adsorption isotherms data leads to confirmation of the existence of adsorbed organic eluent component enriched above the modified adsorbent.

Section 2 is provided with chemicals, instrumentation and detailed procedures for all experiments performed in this research.

Section 3 was divided into two parts. Part 1 discusses the characterization of bonded silica and Combination of different physico-chemical methods allows almost complete

characterization of packing material and column properties. These include nitrogen adsorption for surface area, pore volume and pore size distribution of both base silica and modified material; Gel permeation chromatography (GPC) for characterization of column porosity; retention of deuterated solvent from corresponding non-deuterated form is used for void volume measurement. These data allow assessment of the total surface area in the column and complete characterization of adsorbent geometry. A novel way to interpret HPLC retention factor is provided which is called surface specific retention factor. Correlation of all mentioned parameters with chromatographic behavior of wide variety of columns is discussed. In Part II, excess adsorption isotherm of the adsorbent surface was measured by minor disturbance method and interpreted using excess bi-Langmuir function which allows the assessment of energetic surface heterogeneity. Energetic heterogeneity could be also assessed from adsorption isotherm and correlated to the bonding density.

1   INTRODUCTION

1.1 Adsorbent surface chemistry

High-performance liquid chromatography (HPLC) column technology has evolved significantly in recent years, and HPLC is the most important instrumental technique for qualitative and quantitative analysis of a wide range of compounds. The column is the only device in the HPLC system which always separates an injected mixture. Column packing materials are the media producing the separation, and properties of the media are of primary importance for successful separations.

Stationary phases for HPLC columns have been widely studied [1]. The majority of HPLC packing is silica-based. Almost all silica-based HPLC packing materials are very uniform spherical porous particles with narrow particle and pore size distributions. Silica gel makes an excellent packing material because it can be easily chemically modified, can be manufactured with predefined particle diameter, pore size and surface area, and it provides high mechanical strength to withstand high pressures [2].

A large number of columns are commercially available in the market. Two distinct characteristics are used for silica-based column classification:

1. Type (monolithic, porous, nonporous)

2. Geometry (surface area; pore volume; pore diameter; particle size and shape; etc.)

All parameters of the packing material are interrelated in their influence on the chromatographic performance of the column.

1.1.1 Silica Types (porous, nonporous, monolithic)

The first and most widely used column packing materials for HPLC separations are classical totally porous particles. Since the very first HPLC separation by Huber in 1964 [3] performed with porous particles of a mean size of ca. 40um, the diameter of HPLC packings have been steadily reduced to 5 or even 3 um or less with a single pore-size distribution. The main benefit of the reduction in particle size was an increase of the column efficiency and a decrease of the analysis time. Usually 3 um particle sizes are strongly recommended for most pharmaceutical applications. Small molecules such as drugs generally are separated with packings having pores in the 80-100 Å range, while larger molecules such as proteins often require particles with pores larger than 200 Å. The inter-particle space is large enough to allow up to 1-3 mL/min flow within acceptable pressure range, for typical column dimensions for 4.6 mm I.D.. The surface area is between 100 and 400 m^2/g to provide for the analyte retention.

To expand the utility of HPLC, several silica particle types other than the popular porous silica microspheres have been developed. In the late 1960s, a second type of medium, superficially porous silica particles of approximately 40 um, was made available as the first material specifically synthesized for HPLC separation. These particles were composed of a solid glass bead core and 1-um outer shell of silica with ~ 1000 Å pores [15]. The thin porous shell of these particles allows very rapid access of large macromolecules to interactive surfaces within the porous structure. The result is that high mobile phase velocities can be used for very fast separations with good column efficiency. The recently commercialized version of a partially porous column is packed with 2.7 um shell particles of silica. It was specially designed to provide very high column efficiency [4]. These shell particles are made of a 1.7 um diameter solid core covered with a 0.5 um thick porous shell. This means that the

volume of the porous silica shell is 75% of the total particle volume. It would be interesting to study the comparison on the effective surface area of the columns packed with the totally porous particles and partially porous particles.

The third type is non-porous packing material. The non-porous silica microspheres have interesting properties for very rapid separations, especially for macromolecules having poor diffusional characteristics. The nonporous packing material is another strategy to increase efficiency by eliminating dual column porosity [5]. In the column packed with porous particles, inter-particle space is about 100-fold larger than pores inside the particles, and liquid flow around the particles is also faster. Both factors lead to the significant band broadening. Furthermore, the elimination of particle porosity dramatically decreases adsorbent surface area, thereby decreasing the column loading capacity. Columns packed with small (1.5um) nonporous particles also require ultra-microinjection volumes and a corresponding increase of detector sensitivity [2].

Generally, bonded silica stationary phases are limited to use at acidic and neutral pH conditions [6] since it has an extreme polarity of its surface unstable to basic conditions [2]. The need for improved chemical stability has led researchers to focus on examining new support materials. Polymeric phase is an alternative to improve the performance of silica-based material. The most common one is styrene cross linked with divinylbenzene. Polymer materials provide wide pH stability, but fall short in mechanical strength [7]. Many organic polymer packings shrink or swell when exposed to different solvents. More recently, "Hybrid" columns having a silica core grafted with a unique silica-organic layer have become available [8,9,10]. Since the internal base silica is unaltered by this manufacturing process, the particle retains the mechanical strength and rigidity of silica providing excellent efficiency; while the silica-organic shell protects the particle from chemical attack. With an improvement

3

in high pH stability and a higher level of chromatographic performance, this type of stationary phase is prepared from a sol-gel synthesis of monosubstituted organofunctional silanes or internal organofuctional bridging disilanes in either a homo-condensation or mixed condensation with tetrathoxysilane [118].

In contrast to conventional HPLC columns, monolith columns are formed from a single piece of porous silica gel. The monoliths can be considered a single large particle of porous material that fills the entire column volume without any inter-particle voids typical of packed columns. These columns exhibit 90% interstitial porosity as compared to 80% in the case of packed columns due to the presence of large through pores. Because of this, the stream of mobile phase cannot bypass any significant length of the bed but must percolate through it. The resulting column back-pressure is therefore much lower. Moreover, these monoliths do not need to be packed into a column since they can be prepared in situ by polymerization. The porous material is often characterized by a bimodal pore size distribution. The large size of this distribution corresponds to the macro- or through-pores [11]. Figure 1-1 shows the porous structure of a Chromolith silica rod, a commercial product from Merck KGaA (Darmstadt, Germany) [12]. Macro-pores in the monolith are between 4000 and 6000 Å in diameter and occupy almost 80% of the column volume.

Monolithic columns have proven to be a very good alternative to particle-packed columns for high efficiency separations in HPLC [13,14]. The high permeability makes it easy the use of high mobile phase velocities. The main advantage is that the efficiency of monolithic columns decreases more slowly than that of packed columns with increasing the flow velocity, hence they can be operated at higher mobile phase velocities with a rather small loss in efficiency [11]. They yield fast analyses and are useful in routine analyses when a high

4

Figure 1-1　　　　　SEM-image of the porous structure of a typical monolithic silica column (left) and enlarged view of the entrance to a macro-pore or through-pore (right) [4]
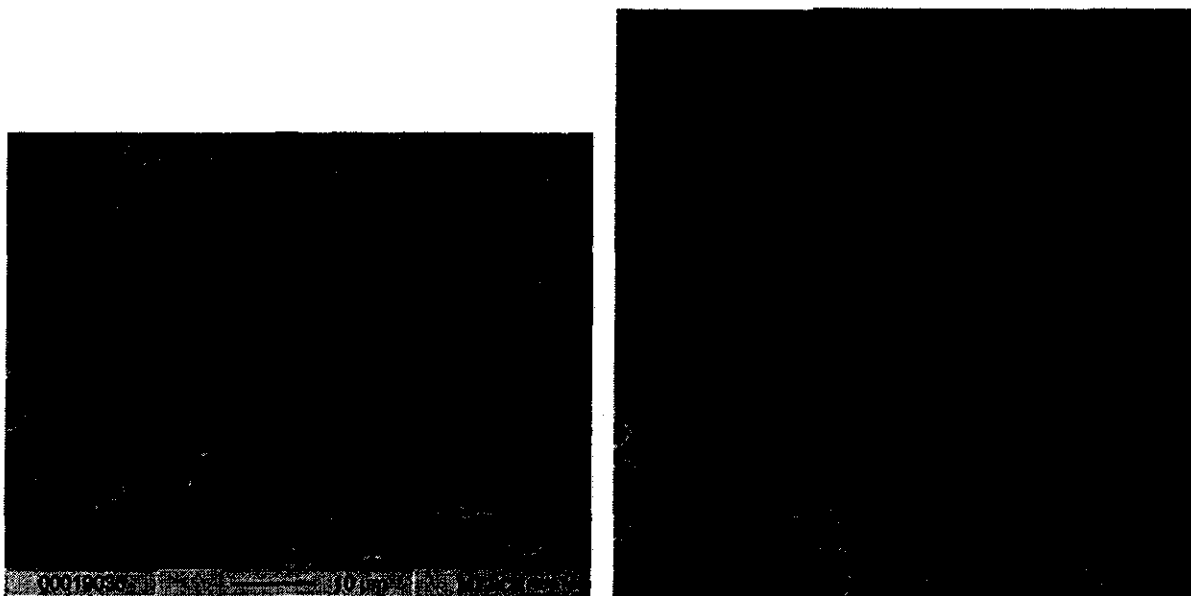
of silica support and its pretreatment, type of the attached ligands and their density, secondary bonding effects and end-capping.

Surface area, pore volume, pore diameter, particle size, and bonding density are important parameters to characterize the adsorbent geometry. For most HPLC silicas, pore diameters are between 60 and 150 Å, surface areas are from 120 to 450 m^2/g, and pore volumes are within the range of 0.5 to 1.2 mL/g. When the alkyl ligands are attached on the silica, this leads to the additional stationary phase variables. Most of the bonded phases used are C_{18} type, and the average bonding density for monomeric phases is above 2.5 $\mu mol/m^2$ [20]. The total content of the modified organic ligand is varied by changing the size of the modifier, specific surface area of the adsorbent and the bonding density. The binding of significant amounts of large alkyl groups, such as C_{18} on the surface area will alter the adsorbent geometry and will influence the mechanism of separation [19]. Bonded alkyl chains occupy volume inside the pore space and are expected to decrease original silica pore volume. A corresponding decrease of the adsorbent surface area and average pore diameter is also expected. The degree of the volume and the surface area reduction depend on the length of the organic ligands and their coverage density. Bass et al [21] studied the effect of surface modification on adsorbent geometry on four different silica gels. Their results clearly show that a decrease of pore volume, surface area, and mean pore diameter was observed with an increase of the chain length of the bonded alkyl moiety. Similar effects of decreasing geometric parameters with increasing bonded alkyl ligand chain length were also observed by other researchers [24,25]. Rustamov et al. [22] determined that the pore volume decreases by 18 uL g^{-1} per CH_2 group.

Study of the surface composition requires the evaluation of the actual surface area available in the column and in essence the mass amount of the solid material packed into the

column. In 2001 Rustamov [22] introduced a non-destructive method for the evaluation of the amount of the packing material in the column. In that study it was shown that the specific pore volume of modified adsorbent measured using low temperature nitrogen adsorption (LTNA) is equivalent to the specific pore volume of the same material packed in the column and measured as the difference of the column void volume and inter-particle volume divided by the adsorbent mass in the column, as illustrated in Figure 1-2. Thus:

$$m_{ads} = \frac{V_o - V_{ip}}{V_p}$$

Equation 1-1

where m_{ads} is the mass of adsorbent in the column; V_0 is the column void volume; V_{ip} is the column inter-particle volume; and V_p is the specific pore volume of adsorbent measured by low temperature nitrogen adsorption (LTNA). Methodologies for the measurement of the correct column void volume and inter-particle volume are also described in the same paper [22]. The easiest method for the void volume measurement is the determination of the retention of deuterated MeOH eluted with the flow of pure regular MeOH. The determination of the inter-particle column volume is based on the measurement of the retention of polymers with sufficiently high molecular weight so that these polymers are completely excluded from the adsorbent porous space. The retention of these polymers eluted with the mobile phase which excludes their interaction with the adsorbent surface (polystyrenes in THF is the good choice) essentially represents the column inter-particle volume. There should be made a correction for the volume of the polymer molecules themselves, which is done by the extrapolation of the retention dependence of polymers with different masses on the cubic root of the polymer mass to the value of zero mass [22].

Figure 1-2   Structure of the adsorbent in HPLC column
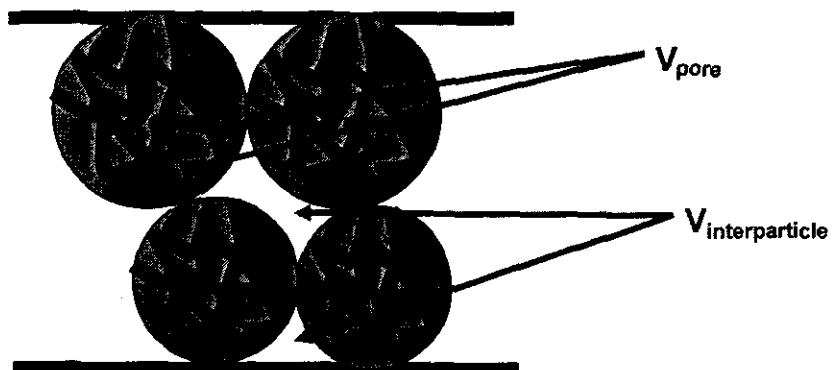
1.1.3   Surface area

Surface area of HPLC adsorbents is arguably the most important parameter, although it is almost never used or accounted for in everyday practical chromatographic work. The adsorbent surface area has a major influence on the stationary phase properties. In theory, HPLC retention is proportional to the total surface area of the adsorbent in the column. Basically, the higher the total surface area, the longer the analyte is retained. Since the retention is directly related to the surface area of the adsorbent, an accurate knowledge of the adsorbent surface area is very important.

The standard method for the measurement of the surface area of porous materials is the application of the Brunauer, Emmet, and Teller theory to the nitrogen adsorption isotherm [16]. BET theory allows the calculation of the amount of nitrogen molecules in the dense monolayer (n_m – monolayer capacity) adsorbed on the measured surface from an experimental adsorption isotherm. This value of monolayer capacity is then multiplied to the area which each nitrogen molecule occupies on the adsorbent surface and divided by the weight of the adsorbent sample used in actual adsorption measurements:

$$S = \frac{n_m \cdot \omega}{m_a}$$ **Equation 1-2**

Where S is the adsorbent specific surface, ω is the nitrogen molecular area, m_a is the mass of adsorbent sample.

The value of the adsorbent specific surface area to which the analyte migrating through the column is exposed presents another complex problem. Nitrogen molecular area is usually assumed to be 16.2 Å^2 [17], although this value was a subject of significant criticism in the last 40 years [18]. Buyanowa and Karnaukhov argued that on hydrophobic surfaces nitrogen adsorption is less localized due to weaker adsorbate-surface interactions and has

more freedom for lateral movement, thus effectively occupying a larger area [18]. This leads to underestimation of the actual surface area of hydrophobic surface, since there are less nitrogen molecules adsorbed in the monolayer and the use of conventional (16.2 Å^2) molecular area will lead to the smaller values of the adsorbent surface area.

It has been discussed before that only the surface area of base silica is a valid measure of the adsorbent surface due to the flexibility and roughness of the surface of chemically modified adsorbent. In the work of Bass and Bratt [19] the numerical values are given for original silica and for same silica modified with different alkylsilanes. Figure 1-3 shows experimental surface area values published in [19] in the graphical form. As one can see, the original silica has the surface area of 420 m^2/g and the surface area of the same silica modified with trimethylchlorosilane is at least 100 m^2/g lower. Other adsorbents modified with longer alkyl-chains show gradual decrease of the surface area almost as a linear function of the number of carbon atoms in the bonded chain. Extrapolation of this line to y-axis results in approximately 330 m^2/g value which is 90 m^2/g lower than calculated using standard BET method with 16.2 Å^2 nitrogen molecular area.

As it was mentioned above, nitrogen molecules will occupy larger areas on hydrophobic surface. It is logical to assume that the ratio of measured BET area on silica sample (420 m^2) to the extrapolated area (330 m^2) will be inversely proportional to the ratio of nitrogen molecular areas on polar silica surface to its area on hydrophobic surface.

$$\frac{S_{N_2(16.2)}}{S_{(extrap.)}} = \frac{\omega_{(hydroph.)}}{16.2}$$
<div align="right">**Equation 1-3**</div>

The value of the area occupied by a nitrogen molecule on a hydrophobic surface estimated from is equal to 20.6 Å^2, which is essentially equivalent to the area estimated by Buyanova

Figure 1-3   Correction of the nitrogen molecular area for adsorbent with alkyl-modified surfaces
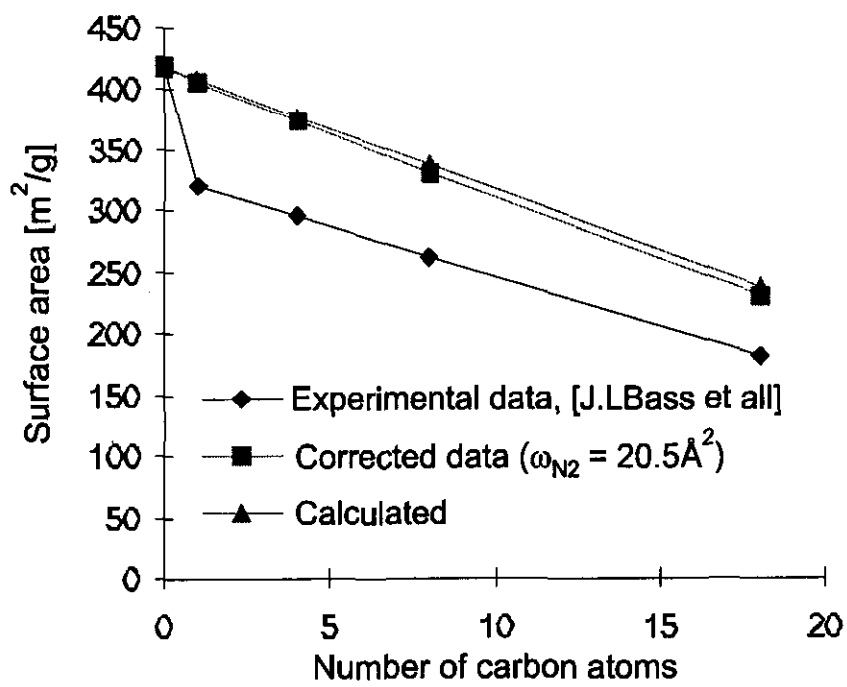
[18] as 20.5 Å^2. If one multiplies the surface area values given by Bass et al. [19] for the modified adsorbents on the ratio of (20.5/16.2), which is essentially the correction for the higher nitrogen molecular area, a nice correlation of original silica and corresponding modified silicas could be obtained as it is shown in Figure 1-3 as corrected data and the sharp discontinuity is eliminated. There is no more significant drop of the surface area between silica and silica modified with smallest possible ligand, and there are gradual linear decrease of the surface area with the increase of the ligand length, which is logical due to the filling of the inner pore space with organic moieties.

1.2   Retention in RPLC

1.2.1   Fundamental HPLC theory

HPLC theory could be composed of two distinct aspects: thermodynamics and kinetics. The thermodynamic factor is responsible for the analyte retention in the column and it determines the peak position on the chromatogram, which is the main discussion point in this thesis; the kinetics part is responsible for the band broadening because of chromatographic zone migration and it determines the width and shape of chromatographic peak. A successful separation could be achieved either by optimization of band broadening (efficiency) or by variation of the peak positions on the chromatogram (selectivity). Practically, the efficiency is more related to column dimensions and adsorbent geometry, while the analyte retention or selectivity is mainly dependent on the intermolecular interaction and is affected by eluent type, composition, temperature and other variations which have continuous functionally variation.

Four basic parameters are commonly used in chromatographic optimization: retention factor (k'), selectivity (α), resolution (R), and efficiency (N).

The retention factor, k', of a compound indicates its retention behavior on a column and is defined as:

$$k' = \frac{V_R - V_0}{V_0} = \frac{t_R - t_0}{t_0} \qquad\qquad 1\text{-}4$$

Where V_R is the analyte retention volume, V_0 is the volume of the liquid phase in the chromatographic system, t_R is the analyte retention time, and t_0 is defined as the retention time of anonretained analyte. Small values of k' show that the compound is poorly retained and elutes near the void volume. Large k' values imply a good separation but downfalls of this are

14

longer analysis times with peak broadening and decreases in sensitivity. Ideal separations occur with a retention factor of between 1 and 5.

Column selectivity, α, is a measure of the relative separation of two peaks and is defined as the ratio of the net retention times of the two peaks:

$$\alpha = \frac{t_{R2} - t_0}{t_{R1} - t_0} \qquad \text{1-5}$$

The aim of LC is to separate components in a mixture into bands or peaks as they migrate through the column. Resolution, R, provides a quantitative measure of the ability of a column to separate two analytes. This measurement is obtained by the retention times and peak widths which are easily obtained directly from the chromatogram. It is a combined measurement of the separation of two compounds which include peak dispersion and selectivity. Resolution is defined as:

$$R = \frac{t_{R2} - t_{R1}}{w_1 + w_2} \qquad \text{1-6}$$

For two peaks to be recognized as separate the resolution should be at least 0.5. Two peaks are seen as completely separate if R is greater than 1.5. The resolution can be improved by lengthening the column but this will also increase the analysis time.

A chromatographic column is divided into N theoretical plates. A thermodynamic equilibrium of the analytes between the mobile and stationary phase occurs within each plate. The efficiency of the column is thus expressed as the number of theoretical plates:

$$N = \frac{L}{H} \qquad \text{1-7}$$

Where L is the length of column packing and H is the plate height.

Efficiency (N) is the measurement of the degree of peak dispersion in a particular column. Poor column efficiency results in band broadening. N is determined experimentally from a chromatogram using the equation:

$$N = 16(\frac{t_R}{w})2 \qquad\qquad 1\text{-}8$$

Where w is the peak width at the baseline.

Efficiency is mainly a column-specific parameter. The geometry of the packing material and uniformity and density of the column packing are the main factors determining the efficiency of particular column [2]. Phenomenologically, an increase of the efficiency can be expected with the decrease of the particle diameter, since the difference between the average size of the pores in the particles of the packing material and the effective size of the inter-particle pores decreases, which leads to the more uniform flow inside and around the particles. More detailed discussion about efficiency was discussed in Ref [2].

1.2.2   HPLC retention mechanisms

Due to the importance and popularity of RPLC, there exists a vast amount of literature in regard to the effects of various experimental conditions on analyte retention. To find optimal chromatographic parameters for a given separation problem and to develop new RPLC columns with improved separation characteristics, there is a need to understand the RPLC separation process. The mechanism of analyte retention in RPLC has been widely studied to predict its chromatographic behavior. Disgreement remains on what is the best theoretical description of analyte retention. The retention of analyte in RPLC is fundamentally determined by its distribution between a liquid polar mobile phase and a nonpolar stationary

16

phase [26]. The expression associating the retention factor with thermodynamic equilibrium constant is dependant on the model selected for the description of the retention process.

An early RPLC retention model was solvophobic theory [31]. It was based on the assumption that the formation of a suitable cavity in the mobile phase to accommodate the analyte molecule was the determining factor in the retention mechanism. Consequently, this model assumed that the retention of the analyte depended essentially on its size and on the surface tension of the mobile phase. The limit of this model became obvious when experimental data showed that retention was also governed by the density and the length of the alkyl chains bonded to the silica surface [32,33]. This was unambiguously interpreted as variation of the phase ratio. Therefore, new models which include the characteristics of both the mobile and the stationary phases were evolved.

Currently, there are two widely used models: partitioning and adsorption. The first one assumes analyte partitioning between mobile and stationary phases; the second one is the adsorption of the analyte on the surface of non-polar adsorbent. Presently, it is unclear whether retention is better described by a partitioning process in which the solutes fully embed themselves into the bonded phase or by an adsorption process at the bonded phase / solvent interface. Furthermore, it is debatable that whether the thermodynamic driving forces for retention lie primarily in the hydrophobic interaction with the aqueous mobile phase or in the lipophilic interaction with the stationary phase.

In partitioning mode, the analyte is transferred from the mobile phase to the stationary phase. In the partitioning-based description of chromatographic retention, the thickness of the stationary phase parameter is essentially hidden and not accounted for, which leads to the significant discrepancies in correlation of retention factors between different columns packed with adsorbents of similar chemistry but different geometry characteristics.

17

An alternative description of HPLC retention is based on consideration of an adsorption process instead of partitioning. Adsorption is an accumulation of one component in close proximity to the adsorbent surface, under the influence of surface forces. Since column packing material is composed of solid porous particles with high surface area and is impermeable for the analyte and the eluent molecules, adsorption is logically a better model for the describing of LC retention compared to partitioning.

Both models have been compared and contrasted in seemingly endless amount of publications [27] and both of them describe analyte retention in very similar mathematical form (simplified) [28]:

$$V_R = V_m + V_s K \quad \text{(partitioning)} \qquad\qquad 1\text{-}9$$

$$V_R = V_0 + SK_H \quad \text{(adsorption)} \qquad\qquad 1\text{-}10$$

where V_m is the volume of the mobile phase in the column, V_s is a volume of the stationary phase in the column, and K is an equilibrium constant, which is an exponent of the Gibbs' Free Energy of the analyte partitioning between these phases. V_o is the total volume of liquid phase in the HPLC column, S is the total modified adsorbent surface area, and K_H is the analyte constant or more specifically the slope of the analyte excess adsorption isotherm at infinitely small concentration (Henry constant).

The first expression states that retention is proportional to the volume of the stationary phase, while the second expression indicates its proportionality to the adsorbent surface. The partitioning model is only applicable for the system with single partitioning process and well-defined stationary and mobile phases. To be able to use Equation (1-9), the volumes of these phases must be defined. The question of the determination of the volume of stationary phase is the subject of significant controversy in scientific literature, especially as it is related to the

reversed-phase HPLC phases [29]. For adsorption model, since adsorption is related to the adsorbent surface, it is possible to consider the analyte distribution between the whole liquid phase and the surface. Using surface concentrations and the Gibbs concept of excess adsorption [30], it is probable to describe the adsorption from binary mixtures without the definition of the adsorbed phase volume. In this case, it is necessary to properly characterize the geometry of the packing materials of the columns.

1.2.3   Partitioning

Partitioning is probably the simplest model of the retention mechanism and the most consistent and understandable description was introduced by Cramers *et al.* [34] in the chapter "Techniques of Gas Chromatography". The detailed mathematical description of the mass balance in the column is illustrated, which has analytical solutions only for binary systems. It assumes the existence of the two phases: mobile and stationary phase. The partition model assumes that the two phases are mutually insoluble. The instant equilibrium of the analyte distribution between mobile and stationary phase is also assumed.

The analyte partition coefficient is (K) defined as:

$$K = \frac{c_S}{c_M} \qquad\qquad 1\text{-}11$$

where c_s and c_m are the equilibrium analyte concentrations in the stationary phase and mobile phase.

The analyte retention factor (k) is defined as the ratio of the total amount of analyte in the stationary phase (q_s) to the total amount of analyte in the mobile phase (q_m):

$$k = \frac{q_S}{q_M} = \frac{V_S c_S}{V_M c_M} = \frac{V_S}{V_M} K \qquad 1\text{-}12$$

The mole fraction of the analyte in the mobile phase (R_f) could be wriiten in the form as:

$$R_f = \frac{q_M}{q_s + q_M} = \frac{1}{1+k} \qquad 1\text{-}13$$

and is regarded as the retardation factor. It is then assumed that R_f could be considered as the fraction time which a component spends in the mobile phase and by multiplying mobile-phase velocity on R_f, the average component velocity (u_c) in the column is obtained:

$$u_c = u\frac{1}{1+k} \qquad 1\text{-}14$$

where u_c is the analyte velocity, and u is the mobile phase linear velocity.

Since $t_R = (L/u_c)$, where L is the column length, Equation 1-14 can be written as:

$$t_R = \frac{L}{u_c} = \frac{L}{u}(1+k) = t_0(1+k) \qquad 1\text{-}15$$

Converting Equation 1-15 into retention volumes using $V_R = F t_R$ and $V_m = F t_0$, where F is the mobile-phase flow rate, and combining Equation 1-12, a well known form is shown as:

$$V_R = V_m + V_s K \qquad 1\text{-}16$$

1.2.4 Adsorption

Adsorption is a process of the analyte concentrational variation (positive or negative) at the interface as a result of the influence of the surface forces. Unlike partitioning, the process of adsorption is a surface phenomenon which occurs at the solid-liquid interface. The solute molecules or adsorbates migrate from the liquid phase to the interface (the adsorptive layer) and displace the physically adsorbed molecules of the solvent. Physical interface between the

20

solid adsorbents and liquid mobile phase is not the same as its mathematical interpretation. The physical interface could be considered to have a thickness of one or two monomolecular layers. In RPLC with chemically modified adsorbents, the bonded layer is a monomolecular layer that is more correctly considered as an interface than the separate stationary phase.

Techniques employed to study the adsorption between the solid and liquid interface can be simplified into two categories: static adsorption from solutions (*e.g.* weight analysis) that operate with an immobile liquid phase and dynamic adsorption (*e.g.* front analysis, minor disturbance) that perform the measurements while the mobile phase percolates through the column at a constant velocity.

1.2.4.1 Static adsorption from solutions

A Classical method of studying adsorption phenomena at the solid – liquid interface was primarily the static measurement, in which the change in concentration of a solute upon addition of the adsorbent to the solution is measured and discrete points on the adsorption isotherm are calculated from this measurement. In this technique, the mass of the adsorbent (m_a) with specific surface area (S) was measured when it was sequentially immersed in a volume (V) of adsorbate solution of starting concentration (c_0). After equilibrium was reached, the resulting concentration of the bulk solution was measured and the excess adsorption value was calculated using the following equation:

$$\Gamma = \frac{(c_0 - c_e)V}{m_a S}$$

1-17

Where Γ is an excess adsorption in mole/m^2, and c_e is an equilibrium adsorbate concentration.

The static method is laborious and uncertain in reaching equilibrium, and it requires a

large amount of solutes and adsorbents for accurate measurements. Most importantly, it tends

to be poorly accurate and moderately precise. Chromatographic methods based on packed

columns have been developed in order to circumvent these problems. The chromatographic

dynamic methods have been proven to be highly accurate. Chromatography allows the choice

between various approaches and techniques to measure adsorption isotherms.

1.2.4.2   Dynamic adsorption from solutions

The development of chromatography as a dynamic separation method based on analyte

adsorption on a solid stationary phase led to the dynamic methods for adsorption

measurements [35]. Two basic methods for measurement of adsorption isotherms were

developed:

1. Frontal analysis method.

2. Minor disturbance method.

The frontal analysis method is the most straightforward in measuring the adsorption

isotherms because of its computational simplicity. Its principle consists in abruptly replacing

the mobile phase pumped into the column with a solution containing a known concentration

of a compound in the same mobile phase while monitoring and recording the composition of

the elute [26]. It is a titration curve since it gives the amount of the compound that is required

to equilibrate the packing material in the column with the new solution. The equilibrium is

reached when a plateau concentration corresponding to the feed concentration is detected at

the column exit.

Experimentally, the flow of pure solvent is replaced with the analyte solution of known

concentration. A typical frontal chromatogram is shown in Figure 1-4. As the concentration

Figure 1-4   Frontal analysis method of determination of the equilibrium concentrations in the stationary phase. The breakthrough curve is presented by the thick solid line. The right stroked areas represent the mass of the compound adsorbed on the surface of the adsorbent
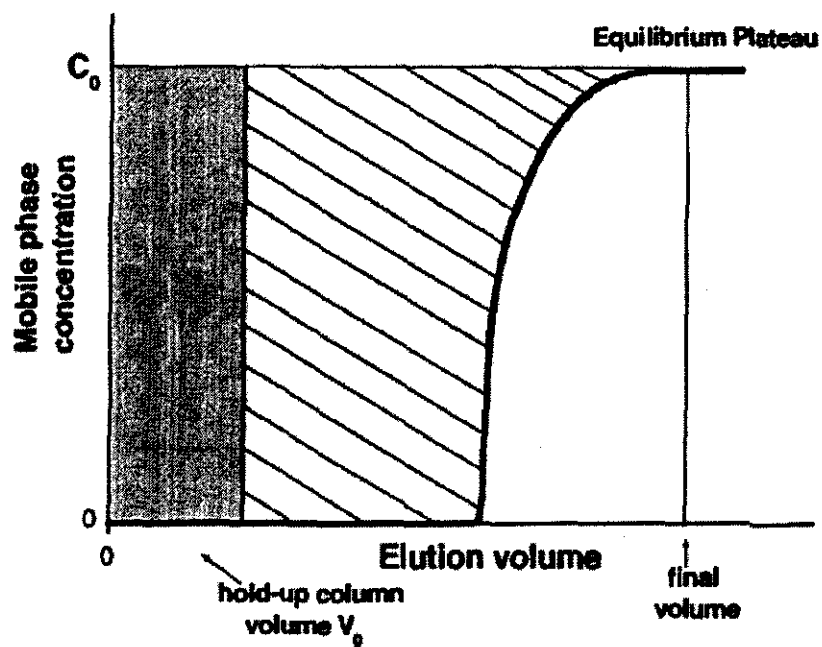
front passes through the column and is detected at the column exit, the flow rate (*F*) is maintained the same throughout the whole experiment. If there is no actual adsorption of the analyte on the adsorbent surface, the front will appear in the detector when it passes through the column volume (V_0), so the retention time of the front will be equal to $t_R = V_0/F$. The amount of the analyte in the column (remaining in the liquid phase) in this case will be $n_0 = V_0 c_0$. If the analyte is positively adsorbed on the surface of the adsorbent in the column, the concentration front will elute from the column later (*t_R*), and the accumulated amount can be calculated as:

$$\Gamma = \frac{t_R F c_0 - n_0}{m_a S} = \frac{(V_R - V_0) c_0}{m_a S} \qquad \text{1-18}$$

Where V_R is the retention volume of the front; V_0 is the column void volume; m_a is the mass of adsorbent in the column; and S is the adsorbent specific surface area.

From Equation 1-18, in order to determine the concentration of the adsorbate in the stationary phase, an accurate estimate of the column void volume V_0 must be obtained.

The acquisition of frontal analysis adsorption data must be made in the broadest possible range of concentrations of the compound. When isotherm data are collected for the purpose of physico-chemical studies such as the study of retention mechanism, two rules must be followed to obtain the highest accuracy possible for the adsorption isotherm: First, the maximum concentration in the injected solution, C_{max}, should be as close as possible to the solubility of the component in the mobile phase. Second, the lowest concentration used for frontal analysis measurements must lead to a symmetrical break-through curve.

The minor disturbance method is one of the most popular methods to measure the adsorption isotherm in a chromatographic system. It has more complex interpretation, which

requires the association of the retention volume to the adsorption isotherm through dynamic mass balance equations [36].

A common way to perform the minor disturbance method is to measure the retention of the mobile phase component over the entire range of mobile phase composition. Two pure solvents (called A and B) that are miscible in all proportions, are mixed at different compositions. Because solvent A adsorbs differently from solvent B on the adsorbent surface at any mixture composition, one can define an excess number of mole n_e of compound A with respect to compound B. A plot of retention volume versus mobile phase composition will show a dramatic change in V_R. Minor disturbance is based on the dependence of the velocity of chromatographic zone on the concentration of the analyte in this zone, which is obtained as a solution of mass-balance equation. For a binary adsorption system, the relationship of the analyte retention volume, VR (c), and its adsorption Γ(c), is given:

$$V_R(c) = V_0 + S\frac{d\Gamma(c)}{dc}$$

1-19

Where, V_0 is the void volume of the HPLC column, S is the adsorbent surface area.

The retention of the minor disturbance peak is proportional to the derivative of the excess adsorption isotherm [37]. Integration of the Equation 1-19 leads to the calculation of the excess adsorption isotherms (Γ) from the experimental data of minor disturbance peaks retention:

$$\int_0^c V_R(c)dc = \int_0^c V_0 dc + S\int_0^c \frac{d\Gamma(c)}{dc}dc$$

1-20

Since the excess amount adsorbed is zero when the column is equilibrated with the pure solvent. After simple transformation, one can get:

$$\Gamma(c) = \int_0^c \frac{V_R(c) - V_0}{S}dc$$

1-21

25

The excess adsorption isotherm could be calculated as an integral of the dependence of the minor disturbance peaks retention on the analyte concentration. Practically, this method is very useful for the determination of adsorption isotherms of the binary eluent system. Column is equilibrated with a specific composition and a small amount of slightly different composition is injected. Because there is difference in the composition between the mobile phase and the injected samples, one disturbance peak was identified as the minor disturbance peak for each binary eluent combination. This procedure is repeated for all compositions (usually 15 to 20 points in the whole range). The dependence is used in calculations of excess adsorption by Equation 1-21.

Both methods allow fast and accurate measurement of the adsorption isotherms only for binary systems when the analyte is dissolved in one single component eluent. As it is in any practical HPLC method with a binary eluent system, the analyte is the third component in the adsorption system. Then theoretically, its isotherm is a surface and the movement of certain analyte concentration zone through the column will be proportional to the slope at this surface directed toward the minimum of the adsorption energy [36]. For the chromatographic system, the two components of binary eluent are present in significant concentrations and the analyte is several orders of magnitude lower concentration. Usually, 10^4 to 10^5 difference is the most common. This allows the assumption that original adsorption equilibrium of eluent components in the HPLC system is not disturbed with the introduction of the small volume of the low concentration of the analyte as a third component. [38].

1.3　Eluent component adsorption

1.3.1　Total and excess adsorption

Adsorption is a surface process, which takes place at the solid-liquid interface. Molecules migrate from the bulk mobile phase to the interface. This process is controlled by the adsorption free energy [47]. The theory of adsorption from solutions onto surfaces of solids has been developed to a far lesser degree. This is due to the fact that adsorption from solutions is determined not only by interaction of the molecules of the components of the solution with the adsorbent and with one another in the adsorption layer, but also by their interactions with the molecules of the bulk solution and within the bulk volume [52]. Thus, the adsorption from solutions is determined not by the entire potential energy of the interaction with the adsorbent, the nature and magnitude of geometry, and nature of the adsorption and structure of the adsorbate molecules, but only by the difference in the molecular field of the adsorbent and the surface and volume solutions, which frequently proves extremely small and can even change sign with changing concentrations [53].

In the case of adsorption of the solution on a solid adsorbent, the molecules of the surface layers interact with the surface of the solid. The chemical nature of the adsorbent plays a vital role in the adsorption of solutions on the solid surface. Adsorption from a binary liquid mixture can be described in terms of the concentration profiles of the two components [45]. The significance of the adsorption isotherm is that it quantitatively describes the equilibrium distribution of a solute between the two phases over a wide concentration range. Determination of the total amount of the analyte adsorbed on the surface requires the definition of the volume where this accumulation is observed, usually called the adsorbed layer volume (Va). In the chromatographic system, adsorbents have large surface areas, and

27

even very small variation in the adsorbed layer thickness lead to a significant variation on the adsorbed layer volume. There is no uniform approach to the definition of this volume or adsorbed layer thickness in the literature [42,43,44].

Another approach to the expression of the analyte adsorbed on the surface is based on the expression of the analyte adsorbed on the adsorbent surface is based on the consideration of the surface specific quantity which has been accumulated on the surface in excess to the equilibrium concentration of the same analyte in the bulk solution. In general, the measured retention is related to the Gibbs surface excess amount rather than to the absolute adsorption of the preferentially adsorbed component [45]. By this way, it can avoid an introduction of any model of adsorbed layer.

In a liquid binary system, the surface of the adsorbent is in contact with individual components of a binary liquid. The composition of the liquid phase changes in an unknown manner from the adsorbent surface to the bulk liquid [48]. An accumulation of the solute is accompanied by the corresponding displacement of another component (solvent) from the surface region into the bulk solution. At equilibrium, a certain amount of the solute will be accumulated in the immediate vicinity of the surface in excess of its equilibrium concentration in the bulk solution, as shown in Figure 1-5 [28]. Everett [50,51] developed a strict definition for the excess adsorption based on the experimentally observed for binary mixtures. Kazakevich et al. [44] had a detailed description of the excess adsorption by the analyte equilibrium concentration derived from mass-balance equation.

Two assumptions were set:

1. Liuqid is uncompressible, or molecular volumes of the solution components are constant.

Figure 1-5   **Schematic of the excess adsorption description [28]**
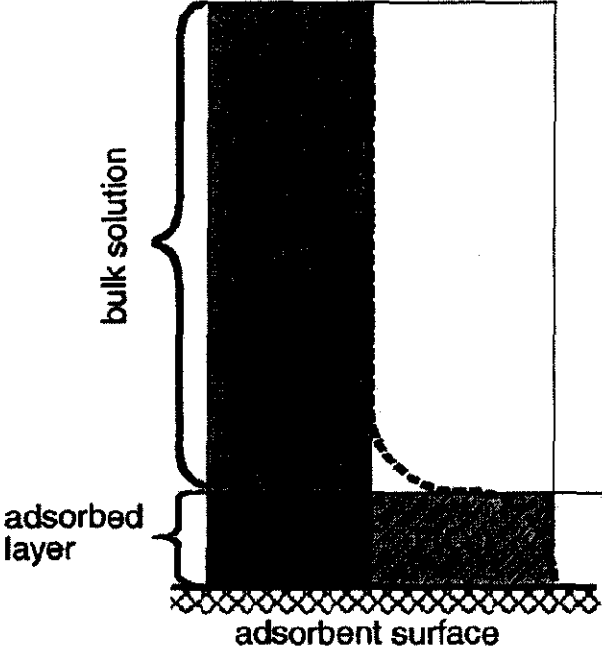
2. Adsorbent surface is impermeable and represents a physical boundary introducing adsorption forces into the liquid phase adjacent to that surface [50].

Excess adsorption (Γ) of a component in a binary liquid system is defined from a comparison of two static systems with the same liquid volume V_0 and adsorbent surface area S. In the first system, the inactive adsorbent does not exert any surface forces in the solution and the whole adsorbent surface is considered to be inert. The original concentration c_0 is uniform throughout the whole volume of the liquid phase. The second system is with the active adsorbent surface and the analyte (organic modifier) is preferentially adsorbed. Therefore, the analyte's amount in the bulk solution is decreased. c_e is the analyte equilibrium concentration in the bulk solution after adsorption, which can be only measured in the bulk solution. Since c_e is less than c_0, the amount $V_0 c_e$ is smaller than the original quanity n_0 due to its accumulation on the surface. The difference $V_0 c_0 - V_0 c_e$ is the excess amount accumulated on the surface on the top of what was present from the equilibrium solution.

This excess amount is usually related to the unit of the adsorbent surface and defined as Γ:

$$\Gamma(c_e) = \frac{V_0}{S}(c_0 - c_e) \qquad \text{1-22}$$

Equation 1-22 can be used for the calculation of the surface-specific excessively adsorbed amount from the original analyte concentration and the equilibrium analyte concentration. It is only applicable for binary system (analyte-single component mobile phase). A similar expression could be derived if it is assumed that the adsorption of the analyte does not disturb the equilibrium of the binary eluent system.

1.3.2   Excess adsorption of the eluent components

Eluent component adsorption has been investigated for many years and many experimental adsorption isotherms have been reported in publications for common solvents used in HPLC [39,40,41]. It is generally recognized that the type of organic eluent modifier plays dominant role in separation selectivity [49]. But the mechanism of its influence on the analyte retention is a subject of intense investigation. The important part of this mechanism is the adsorption of the eluent components on the adsorbent surface. In RPLC, the eluent modifier plays the same role in the adsorption process as do the analytes. They are all part of the same multi-component solution and their excess adsorbed amounts are not independent of each other. In other words, to understand from a fundamental point of view of the distribution of one analyte at infinite dilution between the adsorbed phase and a bulk binary solution, one must understand the excess adsorption of the organic modifier as well.

The connection of HPLC retention with adsorption phenomena is the key for the interpretation of the retention mechanism. The general concept is based on the assumption of instantaneous adsorption equilibrium in a dynamic chromatographic system and the solution for the mass-balance equation for a chromatographic column. Significant amounts of eluent components (organic modifier and H_2O) are known to be adsorbed on the bonded stationary phase. Since the organic modifier is preferentially adsorbed richer in organic content than the bulk mobile phase, the composition of the adsorbed layer is always richer in organic content than the bulk mobile phase.

Many researchers have concentrated on the study of adsorption of the eluent components on the surface of the hydrophobic stationary phase in the last 30 years [42]. McCormick and Karger [54] reported excess adsorption isotherms of H_2O-organic mixtures and discussed different methodologies of their measurements. The methods applied for

adsorption measurements were frontal chromatography [40,45,55,56,57,58], retention of deuterated eluent components [39,59,60,61,62], and introduction of a minor disturbance into the equilibrated chromatographic system [54,59,63,64].

The minor disturbance method is the most common way to measure the excess adsorption isotherms. For a binary dynamic adsorption system, the relationship of the analyte retention volume, VR (c), and its adsorption Γ(c), is given as:

$$V_R(c) = V_0 + S \frac{d\Gamma(c)}{dc}$$ 1-23

This expression describes the analyte retention in a binary system using only the total volume of the liquid phase in the column, V_0, and the total adsorbent surface area S as parameters and the derivative of the excess adsorption by the analyte equilibrium concentration.

In the isocratic mode, the column is equilibrated at a given composition of the eluent. Any small amount of the mixture of the eluent components with a slightly difference in the concentration compared to the eluent is injected in the column. This introduces a minor disturbance in the system. A minor disturbance peak will have the retention volume defined by Equation 1-23. The calculation of the excess adsorption is described in Equation 1-21.

The void volume (V_0) was calculated from the minor disturbance peak retention dependence of a binary eleuent composition. Since excess adsorption of pure component is equal to 0, the integration of the dependence through the whole concentration range was shown as:

$$V_0 = \frac{\int_{c=0}^{c=max} V_R(c)dc}{C_{max} - C_{min}}$$ 1-24

Kovats and his co-workers [39,65,66] was the first to demonstrate that acentonitrile forms an absorbed layer of significant thickness on the surface of the stationary phase. Their

32

interpretation of the experimental results suggested a formation or an approximately 15 Å thick layer of MeCN on the adsorbent surface. They had shown that the thickness of this layer is almost the same for two different reversed-phase adsorbents: 3,3-dimethylbutyl-dimethylsiloxy- and ethyl-dimethylsiloxy- modified silicas [66]. Rustamov [22] and LoBrutto [44] undertook a systematic study of this phenomenon and they found principal differences in the adsorption behavior of the most common HPLC organic eluent modifiers: MeCN and MeOH. MeOH forms only a monomolecular layer on the surface of the reversed-phase adsorbents, while MeCN forms a multi-molecular adsorbed layer of significant thickness up to 1.5nm. An introduction of the adsorption-partitioning retention model has brought up for the third component of the dynamic adsorption system when $MeCN/H_2O$ was used as an eluent [44]. This model summarized that the analyte must partition into the adsorbed MeCN layer and after that it can adsorb on the surface of the stationary phase. In $MeOH/H_2O$ eluent, the retention of the analyte only has the adsorption character.

Typical excess adsorption isotherms of MeCN and MeOH from H_2O on the surface of reversed-phase silica are shown in Figure 1-6. The excess isotherm can be employed to represent the variation of an excessively adsorbed amount of organic solvent with the variation of the equilibrium concentration of this solvent in the mobile phase. In each point of the isotherm, the difference between the amount of organic solvent adsorbed on the stationary phase and the amount of solvent calculated from the volume of the adsorbed phase is shown [28]. The isotherms show slight negative excess at high organic concentration. This indicates a preferential adsorption of H_2O and it is an indication of the presence of accessible residual silanols. The adsorbed layer has a finite volume or finite thickness. When the concentration of the organic solvent in the binary mobile phase increases, the excess amount of this solvent decreases in linear manner. It is caused by the effect of the adsorbed phase filling [28].

Figure 1-6 **Typical excess adsorption isotherm of MeCN and MeOH from H_2O on the surface of reversed-phase silica**
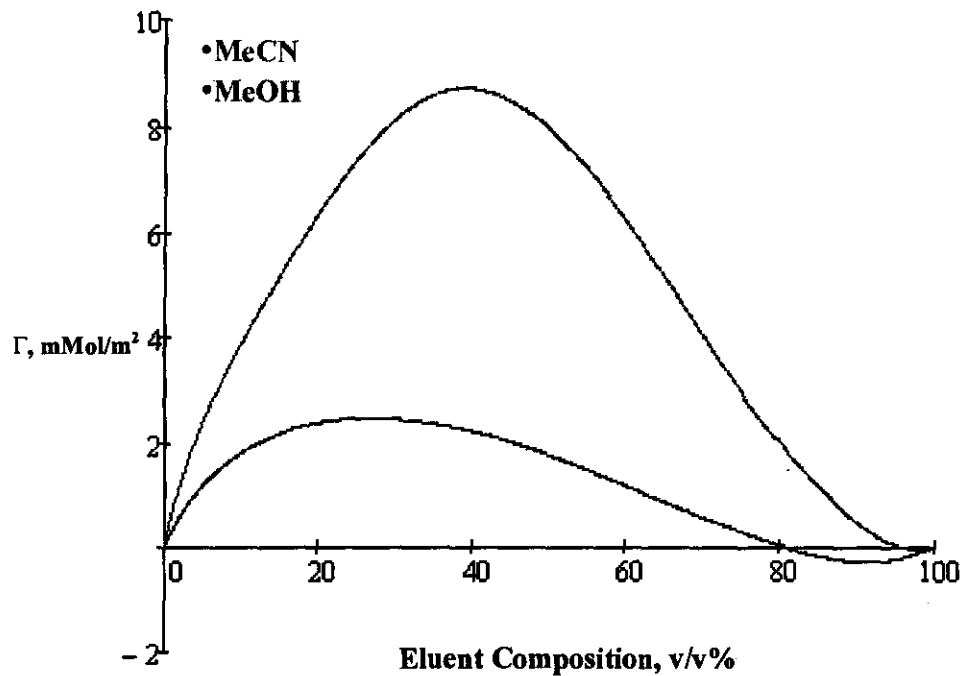
In the region of very high organic modifier concentration, it is possible to assume that the adsorbed phase is completely filled with the organic modifier (MeCN or MeOH). So the following expression for only this region on the isotherm could be written as:

$$(c_e V_a + \Gamma(c_e)) = V_a \qquad 1\text{-}25$$

Where c_e is the organic modifier equilibrium concentration, V_a is the hypothetical adsorbed layer volume, $\Gamma(c_e)$ is the excess adsorption, V_m is organic modifier molar volume. If the layer is not completely filled up with the organic modifier molecules within this concentration region, an additional degree of freedom in the excess adsorption variation with equilibrium concentration still exists, and then there will be no linear decrease at zero excess with 100% of organic modifier in the bulk solution.

Everett [67] developed a mathematical way to calculate the volume of adsorbed layer. By derivation of Equation 1-25 of the equilibrium constant, V_a can be obtained:

$$V_a = -\frac{d\Gamma(c)}{dc_e} \qquad 1\text{-}26$$

So the volume of adsorbed layer can be interpreted as the negative slope of the excess adsorption isotherm in the linear region. It was derived from the consideration of the adsorption process and not from a prior introduction of the model. The derivative of the excess adsorption isotherm in the region of a complete saturation of the adsorbed layer (maximum negative slope of the isotherm) is equal to the surface specific adsorbed layer volume.

Estimation of the maximum adsorbed layer volume from Equation 1-26 allows the calculation of the total adsorption isotherm. On the basis of the assumption of a complete layer filling in the region of the negative linear slope of the experimental isotherm at high organic modifier content, the excess isotherm can be converted into the isotherm of total

adsorption. The adsorption isotherm of the organic modifier can be calculated as the sum of the excess isotherm and the product of the thickness of the adsorption layer and the concentration in the mobile phase as a function of equilibrium adsorbate concentration as [44]:

$$a(c_e) = V_a c_e + \Gamma(c_e) \qquad 1\text{-}27$$

The Equation 1-27 is the total adsorption isotherm derived from experimentally measurable excess isotherm using the model of adsorption process obtained from the analysis of the experimental isotherm profile.

1.3.3   Heterogenity of the adsorbent surface

The chemical modification of the silica gel by binding organic ligands changes the geometry of the silica support and influences the separation mechanism [46]. However, the retention mechanism depends on factors such as surface homogeneity and orientation, dynamics or conformation of the chemically bonded phase [47]. In, RPLC, the type of bonded ligands, coverage density and surface homogeneity with the presence of accessible silanols are the most important parameters which determine the chromatographic properties of the packing materials [68,69]. Although all chromatographers realize that the surfaces of packing materials are somewhat heterogeneous and that this defect may explain numerous difficulties, there is few sound and quantitative answers to explain the heterogeneity of modern RPLC columns. There are no doubts that RPLC materials exhibit heterogeneous surfaces. There are three sources of energetic heterogeneity for the RPLC adsorbents:

1. Active impurities in silica. The silica surface has embedded inorganic impurities (e.g., aluminum, iron, boron, sodium), and it is rough down to the molecular level.

2. Highly polar or ionic compounds trapped in the bonded phases.

3. Accessible residual silanols. The silica surface is sprinkled with a finite density of nefarious silanol groups, which is most important factor determining the heterogeneity.

Retention in RPLC is governed by the hydrophobic effect, i.e. the interaction between organic bonded ligands and the solute [47,70]. Chemical modification of the silica gel surface allows preparing well-defined stationary phase. Despite the derivatization process of the silica gel, the residual silanols are always present in the structure of the stationary phase. The presence of residual silanols can have a negative influence on the separation of polar analytes, especially basic compounds.

The elution of silica based reversed-phase phase packing materials starts with silica surface modified with alkyl silanes to achieve hydrophobicity for separation of organic analytes. Increase of complexity of studied mixtures led to the need of suppression of unwanted polar interactions mainly associated with the influence of residual silanols and active impurities in silica. Most modern adsorbents are based on high purity silica, essentially eliminating "hot spot" effect related to silica impurities. But the high density of silanols on the silica surface (4.5~5 group/um^2) [2] is known to present significant problem since the maximum achievable bonding density for dimethylalkylsilanes are 2.5 group/um^2 [2]. This means that half of the original surface concentration (from 2 to 2.5 group/um^2) of silanols remains on the surface. The majority of these residual silanols are shielded by thick dense layer of bonded alkanes. Although, depending on the bonding density distribution and topology of silica surface, these silanols are accessible for analytes. Presence of the significant quantity of accessible silanols causes tailing of polar or ionizable analytes and forces chromatographers to use ion-paring reagents or other generally unwanted mobile phase additives.

37

Silanols have acidic nature, but their ionization constants are highly dependent on the surface environment and on silica purity. Residual silanols are ionizable with varying pKa (due to amorphous matrix of silica) from 4 to 7. Protons are known to be able to tunnel through 6 to 90 Å thick organic bonded phase layer [2], which makes possible the formation of the effect of underlying negative charge on the surface (pH dependent effect). Proton donor ability of the surface silanols is believed to be the source of peak tailing for analytes with proton acceptor functionality (usually basic analytes). The presence of impurities [71] in bulk silica decreases the silanol pKa, and decreases the hydrolytic stability of bonded phases.

The lack of symmetry of peaks in RPLC has long been explained by the surface heterogeneity of the adsorbent, more specifically, to the presence of undesired, isolated silanol groups within the bonded alkyl layer [74,75]. These silanol groups would be particularly active under pH conditions leading to their ionization. Then, the ionic surface could strongly interact with basic or cationic analytes, resulting in an excessive retention and a peak tailing that impedes their satisfactory detection. The pH range within which these residual silanols are active depends on the column, essentially on the nature of the solid support, the density of the bonded chains, and the end-capping of the support. The mere presence of residual silanols may not suffice to completely explain the origin of peak tailing in chromatography [76]. Many weakly basic, acidic and neutral compounds exhibit also a degree of band tailing [77]. The interaction between silanol groups and these compounds are too weak to explain these unsymmetrical peaks and their excessive retention. Although this may be controversial, there are still strong reasons suggesting that the origin peak tailing in RPLC is in the heterogeneity of the structure of the alkyl-bonded phases [78]. Guiochon explained that the analyte can easily penetrate the "collapsed" alkyl-bonded layer into the regions where the area of contact with these chains is much larger. It brings a quasi-partition configuration with a increased

adsorption energy and affect considerably the band because it reduces drastically the concentration range within which the isotherm is linear.

Even though heterogeneity plays an inevitable role in the separation of RPLC, little or no interest has been devoted to the structure of the bonded alkyl layer in connection with this surface heterogeneity. Most conclusions originate from the analysis of chromatographic data that were obtained at infinite dilution, hence under linear conditions. Tests based on linear elution of weak or strong basic compounds reveal high-energy sites of interaction between these bases and the acidic silanol groups, leading to an excessively high retention (thermodynamic contribution) or to strong peak tailing (thermodynamic or kinetic contributions). The slow kinetics of the desorption process from these high-energy silanol sites has been the most widespread physical interpretation of peak tailing in chromatography. It is only recently that chromatographers begin to understand how pervasive it is for the contribution of surface heterogeneity to elution profiles at low concentrations [72,73].

The advancement of chemical analyses requires a better understanding of surface heterogeneity of RPLC materials. The achievement of this goal requires the application of suitable methods to characterize the surface of the packing materials. Recent investigations based on the measurement of excess adsorption have brought out new insights of the surface heterogeneity. Guiochon and his research groups did excellent work on the study of surface heterogeneity based on excess adsorption of the organic eluents on different types of bonded phases [78,79,80,81,82]. They investigated the effect of the length of the bonded alkyl chain on the adsorption behavior of low molecular weight compounds, including the number of types of adsorption sites and adsorption energies. Unfortunately, the degree of heterogeneity of an adsorbent that they have estimated is not a characteristic of the column, it depends on

the probe they choose, which was explained very clearly in the work of Guiochon [78,79,80,81,82].

1.4   HPLC analyte retention

The RPLC retention of a compound is determined by its polarity and experimental conditions: mobile phase, column, and temperature. The analyte nature in the mobile phase is also the factor that affect the retention mechanism. Eluent pH influences the analyte ionization equilibrium. Eluent type and composition affect the analyte salvation. These equilibria influence the analyte retention and selectivity, which is the primary concern in the development of the separation methods for most pharmaceutical compounds.

1.4.1   Effect of eluent type and composition

An important parameter contributing to the retention of a solute in RPLC is the mobile phase. Mobile phases commonly used in RPLC are hydro-organic mixtures. The mobile phases are based on a polar solvent, typically H_2O, to which a less polar and stronger solvent such as MeCN or MeOH is added. Solvent selectivity is controlled by the nature of the added solvent. Retention is preferably adjusted by changing mobile phase composition or solvent strength. In RPLC, retention is less for stronger, less polar mobile phases. In other words, increasing the fraction of the organic solvent increases the solvent strength and allows for elution for the species in a mixture, resulting a smaller analyte retention factors or retention volume. Solvent strength depends on both the choice of organic solvent and its concentration in the mobile phase.

The general model of reversed phase retention is based on molecular interactions occurring between the solute and components of the mobile and stationary phases [83,84,85,86,87,88]. In the mobile phase, it is believed [89] that the dominant interaction between the solute and H_2O is solvophobic expulsion of the solute from the mobile phase into

41

the stationary phase. The organic modifier may also influence retention through its interactions with the solute, H_2O molecules, and the stationary phase.

Not only the concentration of the organic modifier, but also the type of organic modifier affect the mobile-phase strength. Given the same volume percentage (v/v %), the solvent strength of the most common organic eluents in RPLC would be: MeOH < MeCN < THF, which is only an approximation because the retention of an analyte in different organic modifier may depend on many parameters leanding to different interactions of the analyte with the solvent or with the bonded phase.

The principle in the difference of the analyte retention behavior from the different organic modifiers was recently studied by Kazakevich et al. [44]. In a binary eluent system, an adsorbed organic phase with finite thickness and composition different from the bulk mobile phase is preferentially accumulated near the surface of the bonded phase. It has been experimentally shown that the organic modifiers adsorb selectively on the RPLC stationary phase [93,94,95,96]. MeCN is definitely more strongly adsorbed than MeOH and may compete with the compound for adsorption on the stationary phase. This explains partly why the elution time is systematically reduced when MeCN is used as the organic modifier. The increase of solubility of the solute in MeCN may also contribute to the loss of retention [97].

It has been demonstrated that changes in the type of organic modifier do not have pronounced influence on the interactions of the solute in the mobile phase [87]. This effect is presumably due to the dominance of solute-H_2O interactions over solute-organic modifier interactions. Consequently, changes in selectivity for a given stationary phase, as a function of different organic modifiers, can most likely be attributed to the interactions that occur between the solutes and the adsorbed organic layer on the stationary phase [90,91,92].

Assuming only analyte-eluent competition for the stationary phase surface and in the absence of any secondary equilibria, one can write [2]:

$$k = \frac{S}{V_0} K \qquad\qquad 1\text{-}28$$

Where K is a thermodynamic equilibrium constant, which can be expressed as:

$$\Delta G = \Delta G_{analyte} - \Delta G_{eluent} = RT \ln K \qquad\qquad 1\text{-}29$$

Where $\Delta G_{analyte}$ is the free Gibbs energy of the analyte interaction with adsorbent surface and ΔG_{eluent} is the corresponding free Gibbs energy for the eluent.

Equation 1-29 can be transformed into:

$$K = \exp(\frac{\Delta G_{analyte} - \Delta G_{eluent}}{RT}) \qquad\qquad 1\text{-}30$$

Therefore, increasing the concentration of the organic modifier generally results in an exponential decrease in the analyte retention volume.

The dependence of retention factor on the organic modifier composition is a subject of controversy. It is generally accepted that the logarithm of the retention factor shows linear variation with the volume fraction of the eluent composition [98,99], while there were many reports which declare a quadratic relationship [100,101,103,104] and implies that the deviation from the linear relationship will be more pronounced at high concentration of the organic modifier. Synder et al. [102] introduced a simiplified semi-empirical equation to describe the influence of the eluent composition on the analyte retention in RPLC:

$$\log(k) = \log(k_w) - S\Phi \qquad\qquad 1\text{-}31$$

Where k_w is the extrapolated analyte retention factor in pure H_2O, Φ is the volume fraction of the organic eluent modifier, and S is the slope of this linear function specific for a particular organic modifier used and the nature of the solute, especially the molecular weight.

43

In all, analyte retention in organic eluent is the superposition of different process: partitioning and adsorption. The volume of MeCN adsorbed layer depends on the eluent composition, which may provide the explanation for the nonlinear behavior of the logarithm of the retention factors versus the eluent composition.

1.4.2   HPLC Retention factor

The traditional representation of HPLC retention is based on the retention factor (k') [105], which in turn is associated to the thermodynamic equilibrium constant [2]. As a very rough approximation, the chromatographic retention process could be described on the basis of an equilibria of the analyte distribution between the mobile phase and stationary phase. The retention factor is proportional to the free energy change associated with the chromatographic distribution process. It is also related to the partition coefficient. Thus, solute retention is affected by the thermodynamics of distribution between the stationary and mobile phases. The compositions of mobile phase determine the retention volume of solutes. For RPLC column, the major constituent is a highly polar solvent (e.g., H_2O), and the less polar solvents of organic modifier (e.g., MeOH, MeCN, etc.) are added to control the hydrophobic nature between solute and coated stationary phase.

The variations of the mobile phase composition, temperature, pH are the most studied parameters in HPLC research [107,108,109]. The other intensively developed aspect of HPLC is the adsorbent surface chemistry or the variation of the surface interactions by chemical modification of the surface of solid porous material [110,111]. It is interesting to note that: in more than 30 years of intensive research, the analyte retention variation with mobile phase composition, pH, temperature, and buffer concentration can generally described in functional

form [28], although the use of the same functions for the prediction of the retention of another analyte in general does not work. While the functional description is somehow possible for the mobile phase related parameters, the description of the influence of adsorbent parameters on the analyte retention is still only phenomenological.

Retention factor is a convenient dimensionless parameter routinely used for comparison of the retention properties of different columns [106]. The widely used retention factor of a solute, k, is the ratio of a reduced retention volume, and the retention of a substance believed to traverse the column with the same velocity as that of the mobile phase, V_0, which is shown in Equation 1-4. Obviously, the retention factor is not suitable to report the retention data for the same compound on the same type column (e.g. C_{18}) from different manufacturers. A series of chromatographic methods such as Tanaka test, Engelhardt test, Galushko test, Walters test were developed to characterize C_{18}-type stationary phase using the parameter of retention factor [114,115,116]. The illustration on the variation in the retention of the same analyte on the C_{18}-type adsorbents still remains unclear. Comparison of the analyte retention at the same mobile phase conditions on different reversed-phase columns usually shows significantly different results even for the adsorbents with identical surface chemistry, such as octadecyl-modified HPLC adsorbents [112]. Most of C_{18}-type stationary phases for HPLC, although slightly different from each other, show very similar methylene selectivity, which indicate that their hydrophobicity is essentially the same [113].

2   EXPERIMENTAL

2.1   Principles

A comprehensive understanding of the heterogeneity of the adsorbent surface requires complete physical characterization of the adsorbent properties in terms of geometry (pore volume, surface area), adsorption activity (excess adsorption isotherm), and comparison with their chromatographic behaviors.

The following adsorbent properties were characterized:

1. Adsorbent surface area

2. Adsorbent pore volume, pore size and pore size distribution, and bonding density.

Colum packed with the studied adsorbents were characterized for the following:

1. Column void volume

2. Column inter-particle volume

3. Isotherms of MeCN adsorption from H_2O

4. Isotherms of MeOH adsorption from H_2O

The following methods were used in this study:

1. Low termperature nitrogen adsorption: for the determination of surface area and pore size dist.

2. Gel permeation chromatography: for the determination of the column inter-particle volume.

3. Minor disturbance method: for the measurement of the adsorption behavior of MeCN and MeOH on the surface of RPLC adsorbents.

4. Elution chromatography: for the comparison of the specific surface retention factor and the traditional retention factor of the probe analytes on the selected adsorbents in RPLC.

2.2   Determination of geometric parameters of the stationary phase

2.2.1   Columns

Six commercial columns with different geometry and surface chemistry characteristics were used in this study. Names, dimensions and other parameters provided by manufacturers are shown in Table 2-1. The Halo columns were from Advanced Materials Thechnology (Wilmington, DE, USA). The Allure Columns were purchased from Restek (Bellefonte, PA, USA). The YMC Pack Pro columns were provided by YMC (Kyoto, Japan). The Gemini columns were obtained from Phenomenex (Torrance, CA, USA). The Xterra and Xbridge columns were supplied by waters (Milford, MA, USA).

In this set, columns of principally different nature are included. Allure and YMC columns are conventional silica-based porous materials modified with octadecylsilanes. Halo is also silica-based material, but its spherical and very uniform particles consist of the solid (nonporous) silica core with 1.7 u diameter and porous silica layer with 0.5 u thickness created on this core, which is illustrated in Figure 2-1 [119]. This presumably increase surface accessibility by decreasing molecular traveling distance inside porous particles, while it is also decrease the material surface area.

Table 2-1   **Column parameters**

Name	Manufacturer	Dimensions (mm)	Particle size (um)
Halo-C_{18}	Advanced Materials Thechnology	50 x 4.6	2.7
Allure-C_{18}	Restek	150 x 4.6	5.0
Xterra-C_{18}	waters	150 x 3.0	3.5
YMC Pack Pro C_{18}	YMC	50 x 4.6	3.0
Gemini C_{18}	Phenomenex	100 x 2.0	3.0
XBridge C_{18}	waters	150 x 3.0	3.5

Figure 2-1 **Graphical representation of HALO adsorbent**
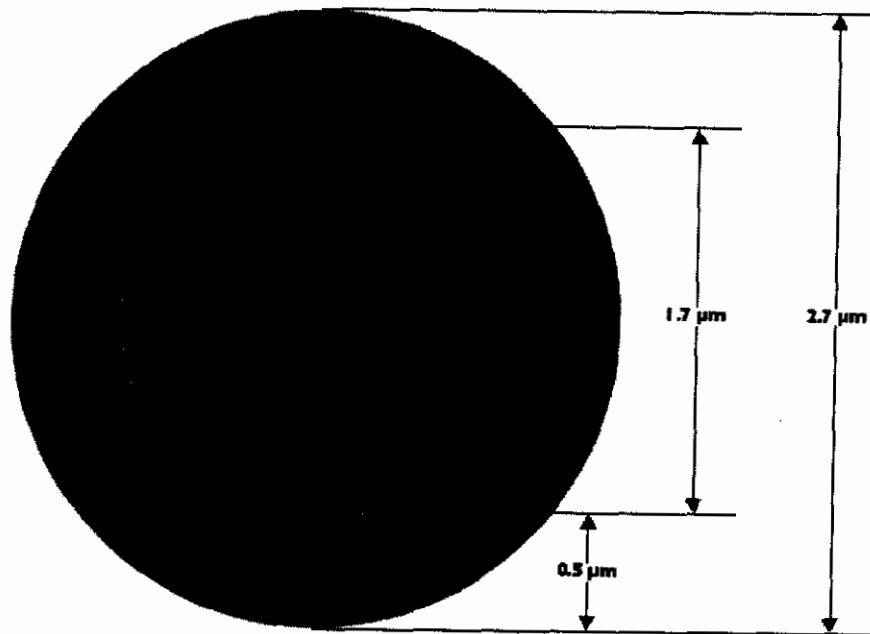
Xterra is composite material made by co-synthesis of silica matrix using tetraethoxysilane and methyryethoxysilane which allow inclusion of methyl groups in the body of silica base material. Presence of the methyl groups on the silica surface results in the decrease of the total number of silanols, thus after chemical modification of the surface there are less residual silanols left. XBridge is the further development of Xterra concept, were methyl groups are substituted with ethyl bridges, which presumable should increase the physical strength of the base material and leave even less unreacted silanols on the surface [117].

Gemini is another example of a composite material, where regular porous silica is used as a base core and a layer of organic-embedded silica is synthesized on the top of silica core. This design allows for the silica-like mechanical properties of base material while similarly decreasing the number of residual silanols [118].

2.2.2   Adsorbent parameters

The bulk unmodified silicas and modified silicas of the identical batches as in the packed columns were characterized in this study. Determination of bonding density of the modified stationary phase of Halo, Allure and YMC columns are discussed in 3.3 of this dissertation.

2.3   Materials

All solvents used in this study such as acetonitrile (MeCN), methanol (MeOH), and tetrahydrofuran (THF) were HPLC grade from Pharmco (Phillipsburg, PA, USA). H_2O was purified using Milli-Q system (Millipore, El Passo, TX). Deuterated MeCN and deuterated MeOH were obtained from Sigma Aldrich (St. Louis, MO, USA).

Nitrogen gas (zero grade), liquid nitrogen L-240 (reagent grade), and helium gas (zero grade) utilized in LTNA experiments were purchased from Airgas (Piscataway, NJ, USA).

Polystyrene standards with high molecular weights of 194000, 382000, 410000 860000 and 994000 (all narrow molecular weight distribution, r less than 1.05) utilized in column inter-particle volume determination were purchased from Sigma Aldrich (St. Louis, MO, USA).
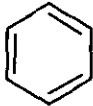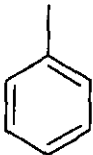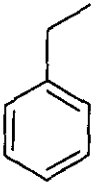
High purity non-polar probe analytes such as benzene, toluene and ethylbenzene used in the retention studies were purchased from Sigma Aldrich (St. Louis, MO, USA). The structure and properties of the test analytes were summarized in Table 2-2. These anlaytes were picked because they are neutral compounds, and only have hydrophobic interaction with the stationary phase without any ionic interactions.

2.4   Apparatus

Nitrogen adsorption measurements for the characterization of bare silicas and modified silicas were performed on Omnisorb model 100CX system (Omnisorb, NJ, USA) using static adsorption mode with full equilibration of each adsorption point. Adsorption and desorption isotherms were measured for each adsorbent. Raw data from the adsorption system were transferred into MathCad 12.0 software and homemade software template was used for the calculation of the adsorbent pore volume, surface area, BET C-constant and pore size distribution.

HPLC experiments were performed with two HPLC systems. The first system was Agilent model 1050 (New Castle, DE) system equipped with 3900E analog interface and PE LC-30 refractive index detector (RI) (Perkin-Elmer Wellesley, MA, USA) and Chemstation

51

Table 2-2   **Structures and properties of the probe analytes**

Analyte	Structure	pKa
Benzene		43
Toluene		41
Ethylbenzene		40

software. The second system was model 1100 system with diode array detector (Agilent, New Castle, DE). All eluents were degassed with a degasser unit (Phenomenex, Torrance, CA, USA).

2.5   General HPLC Procedures

All HPLC experiments were conducted in isocratic mode. System volume was determined by the elution of 0.5uL of deuterated MeOH in MeOH in triplicate using RI detector. Experimental values for the retention were corrected for extra-column volume for these three sets of HPLC systems. Extra-column volumes were obtained by elution of 0.5uL of deuterated MeOH (HPLC with RI detector) and 0.5 uL benzene (10 ppm) respectively with direct connection of column inlet and outlet capillaries. The average retention volume in triplicate was used.

After the completion of each set of conditions with the specific eluent type and composition, the column was cleaned using shock method: cyclic flush with H_2O and MeCN, 2 minutes each with sharp momentary switch between them followed by 15 minutes equilibration at 1 ml/min for the next eluent composition.

2.6   Surface area and pore volume characterization by low-temperature nitrogen adsorption

Bare silica and chemically modified silicas were characterized using the nitrogen adsorption system model 100CX (Omnisorb, NJ, US) by low-temperature nitrogen adsorption (LTNA). The weight of a clean sample vessel was recorded. A sample size of approximately

0.1 g of absorbents were degassed under vacuum (4×10^{-5} torr) either 150°C for 3 h (for bare silica) or without heating (for chemically modified silica). After cooling, the vial was weighed and placed into the adsorption instrument for analysis. An empty sample vessel filled with nitrogen gas was also placed into the adsorption instrument. The pressure of the reference vessel was monitored by the instrument and was determined to be the saturation pressure of nitrogen at 77K. Helium gas was used to calibrate the internal volume of the sample vessel. Static adsorption mode was utilized for all measurements with equilibrium criteria of 0.01% tolerance for nine consequent sampling points. Pore volume was determined from the volume of liquid nitrogen after the completion of capillary condensation in the porous space. Figure 2-2 shows the experimental dependence of the volume of nitrogen adsorbed on the surface at the temperature of liquid nitrogen (77K) versus the relative pressure, including two processes: adsorption and desorption. The relative pressure is the pressure of nitrogen adsorbed at the equilibrium related to the saturation pressure.

In the relatively low pressure region between 0.05 and 0.25, the adsorbed monolayer is complete and used for the calculation of the surface area per adsorbent weight, which is shown Equation 1-2. It is generally assumed that a nitrogen molecule occupies 16.2Å^2 on the polar silica surface. The absorbent surface area is then calculated as a product of the total amount of nitrogen in the monolayer and the nitrogen molecular area (16.2Å^2) [17].

At higher relative pressures above 0.7, a fast increase of the adsorbed amount of nitrogen is observed. This region is attributed to process of capillary condensation of nitrogen inside the adsorbent pores. This increase is observed till the whole pore volume is filled with liquid nitrogen, where a small flat section on the adsorption is observed. This could be used for the accurate determination of the adsorbent pore volume [16].

Figure 2-2   An example of LTNA isotherms of bare silica
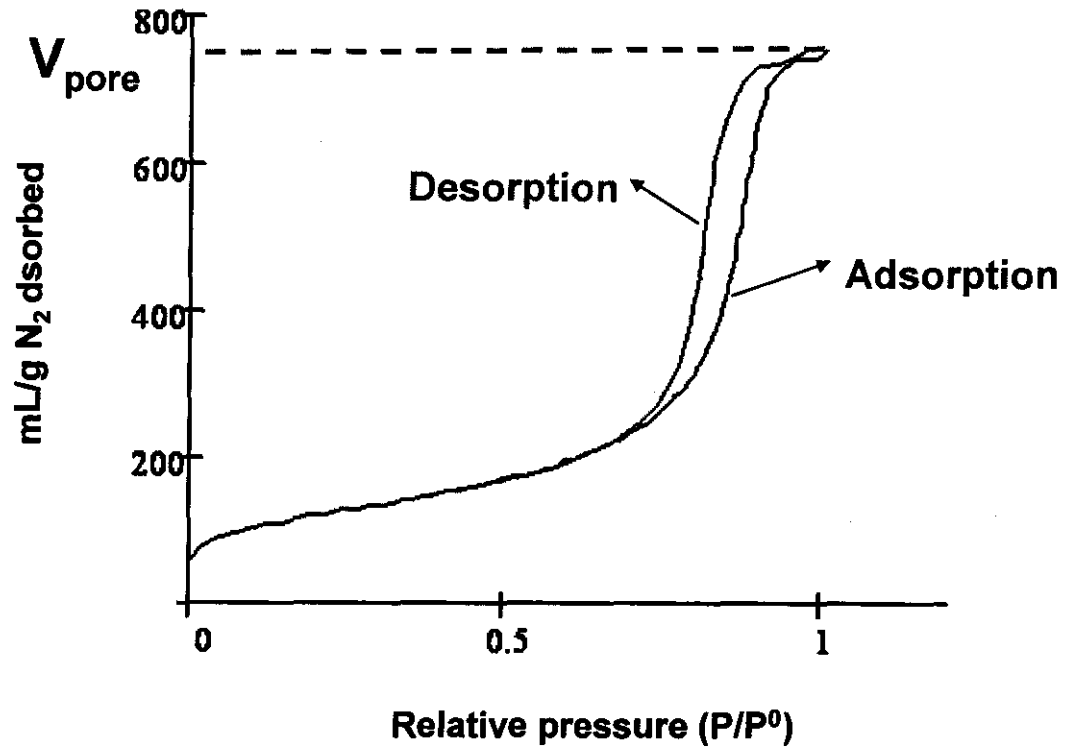
2.7   Mass of modified adsorbent measurement

One column of each type was washed with MeOH and unpacked into the pre-weighed vial. Vial with adsorbent was than set into the oven with 60 °C temperature for 24 hours to allow complete evaporation of the solvent. Temperature was increased to 80 °C for 1 hour and vial was cooled and weighed. Vial was than placed back to the oven for 1 hour and weighed again. This procedure was repeated until constant weight was reached. This unpacked material was then used for nitrogen adsorption and TGA measurements.

2.8   Column characterization using HPLC methodologies

2.8.1   Column inter-particle volume determination by gel permeation chromatography (GPC)

GPC separates polymer molecules based on differences in their molecular size. The separation process is based on the exclusion of the molecules from the porous space of packing material and is dependent on the relative size of analyte molecules and the respective pore size of the absorbent. The inter-particle volume is the volume between packed adsorbent particles within an analytical RPLC column. This measurement requires the use of relatively large polymer molecules which have their own significant volume. Based on the value of their gyration radius, the inter-particle volumes will have additional exclusion from the stationary phase surface. The radius is roughly proportional to the cubic root of the molecular weight, thus the cubic root of the molecular weight should be proportional to the analyte retention volume. A linear relationship between the cubic root of the molecular mass of the polymers

and their retention time is observed [44]. By extrapolation of the linear curve to the zero mass point on the x-axis, the inter-particle volume can be obtained.

A series of high-molecular-mass polystyrene standards molecular weights 194000, 382000, 410000 860000 and 994000 were dissolved in THF. The total exclusion volumes of all the absorbents were acquired by eluting all the standards at 0.5ml/min using THF mobile phase. A UV detector wavelength of 254 nm was employed. The concentration of each polystyrene standard solution in THF was prepared to be approximately 0.1mg/mL. Three injections of 0.2 uL of each standard solution were injected into the column. Figure 2-3 shows the extrapolation of the column inter-particle volume from the plot of cubic root of polymer standard molecular weights versus retention volume.

2.8.2   Excess adsorption and column void volume by minor disturbance method

The excess adsorption isotherms of organic modifiers (MeCN and MeOH) from H_2O on chemically bonded stationary phases were studied, using several different packed C_{18} columns. The isotherms were measured using the minor disturbance method, which is also called the perturbation method [44]. The different mobile phases used in this measurement were prepared by mixing known volumes of H_2O and organic modifier. Each column was successively equilibrated with mobile phase volume fractions of 0, 1, 5, 10, 20, 30, 40, 50, 60, 70, 80, 90, 95, 99 and 100% by pumping at least 50 mL of the solvent mixture. The stationary phases were equilibrated at each eluent composition for 15 minutes prior to the initial injection. The reaction of the system was detected with a refractive index detector. The reference cell of the refractive index detector was equilibrated with pumped eluent at the same

Figure 2-3   **Dependence of the retention volume versus the molecule size**

$y = -0.0004x + 0.3891$
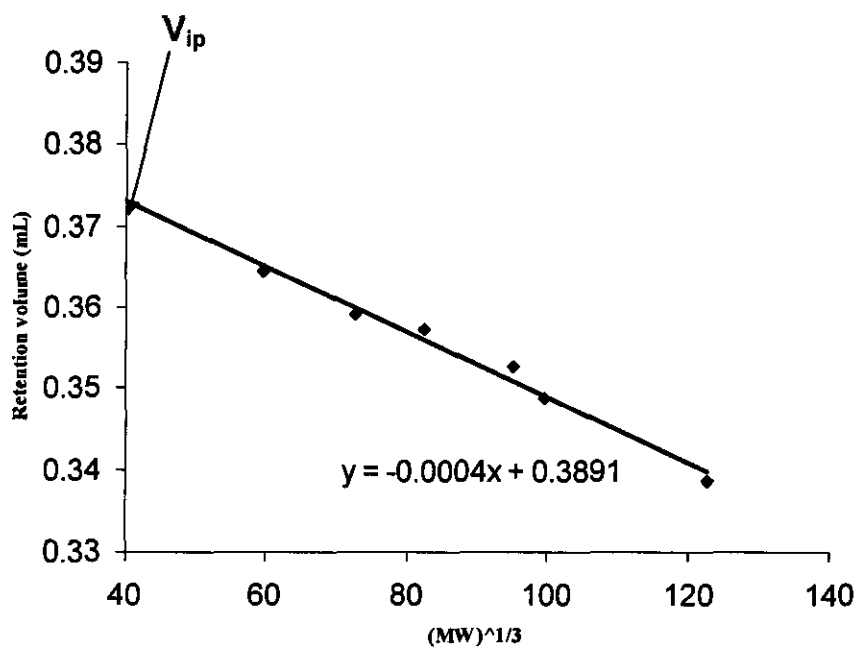
flow rate for 10 minutes or longer until a stable baseline was observed. A small perturbation in a system under equilibrium was recorded by the injection of the mixture with slightly higher or lower concentration of the organic solvent than the plateau concentration. In order to minimize the peak band broadening [23], small injection volumes (0.2 uL to 2 uL) were utilized in this analysis. The retention time of the perturbation peak was measured. Integration of the minor disturbance peak retention volumes throughout the entire eluent composition range led to the column void volume. The flow of the mobile phase was 0.5 mL/min. The retention volume for the asymmetric peak observed in extreme mobile phase composition was estimated from the extrapolation of the peak tail.

Integration of the minor disturbance peak retention volumes throughout the entire eluent composition range leads to the column void volume:

$$V_0 = \frac{\int_{c=0}^{c=max} V_R(c)\,dc}{C_{max} - C_{min}} \qquad\qquad 2\text{-}1$$

The excess amount adsorbed is given by:

$$n(c) = \int_0^c (V_R(c) - V_0)\,dc \qquad\qquad 2\text{-}2$$

2.8.3   Column void volume determination by deuterated components

To ensure the accuracy of the void volume determination by the minor disturbance method, the void volumes of all the stationary phases were also determined by the retention of deuterated organic solvent. Two organic eluents were used: MeCN and MeOH. The void volume was obtained by the retention of deuterated MeCN eluted in the mobile phase of pure

MeCN, and also with deuterated MeOH eluted in pure MeOH. A RI detector was used in this analysis. The columns and the refractive index reference cell were equilibrated in pure organic eluent at a flow rate of 0.5 mL/min. A small volume with 0.5 uL of the deuterated component of the corresponding pumped eluent was then injected into the column in triplicate measurements.

The void volume of the column was produced by the retention volume of the deuterated peak corrected for the system volume [54]. The void volumes of the same column by each of the two solvents were compared and contrasted.

2.8.4   Experimental analyte retention volume determination

The retention volumes of alkylbenzenes (Benzene, Toluene, and Ethylbenzene) at low concentrations were obtained under the mobile phase composition 70/30 (v/v) MeCN : H_2O and MeOH : H_2O. The data acquisition was performed under ambient conditions. A UV detector was employed with the wavelength set at 254 nm. The injection volume was 1 uL on each column performed. The concentration of the injected alkylbenzenes was 0.1 mg/mL which produced a discernible peak was produced at the higher detector sensitivity.. The low solute concentration in the sample produced the symmetrical peaks and thus the retention volumes were measured at the point of maximum concentration in the solute band. The reproducibility of the measured retention volumes, for each analyte on each column, was determined by injecting each analyte three times for a given set of HPLC conditions and the average of the three was used to obtain the retention volume. Relative standard deviation of the averaged retention volumes were less than 2%.

3   RESULTS and DISCUSSION

3.1   Nitrogen adsorption

Each of the unpacked adsorbents was carefully collected and dried to constant weight to determine the actual amount of adsorbent in (Table 3-1) that was packed into each column by the manufacturer. The surface area, pore volume, and pore size distribution (Table 3-2) were obtained by low-temperature nitrogen adsorption measurements of full (adsorption and desorption) isotherms. .

All of the isotherms shown in Figure 3-1 have a very small increase at low relative pressure values, which indicates minimal nitrogen adsorption interactions with hydrophobic surface. The hysteresis loops for the Halo and Allure adsorbents are also at relatively low p/p_s values, which indicate that their pore sizes are smaller when compared to the other adsorbents. The last column in Table 3-2 lists the C-constant values of the BET equation, which were calculated for each of the adsorbents in this study. All these values are between 20 and 22, which, according to Karnaukhov [18], correspond to the adsorption of nitrogen molecules on a polyethylenelike surface or a surface covered mainly with methylene (CH_2) groups. Buyanova [18] suggested that nitrogen will occupy a molecular area of ~20.5 $Å^2$ on that surface type. The surface area values corrected for this larger area value for molecular nitrogen are shown in column 3 of Table 3-2.

In early publications [22,44], the use of the base silica surface for the calculation of excess adsorption isotherms and other surface specific parameters was suggested. This is appropriate for the comparison of the chromatographic and adsorption behavior of analytes on

61

Table 3-2 Adsorbent geometry parameters from full (adsorption and desorption) nitrogen adsorption isotherms.

Adsorbent	S (at 16.2 A^2)	$S_{corr.}$ (20.5/16.2)	V_{pore}	R_{pore} (max)	R_{pore} (median)	R from 2V/S	Distrib. assymmetry	C BET const.
	m^2/g	m^2/g	mL/g	Å	Å			
Halo-C_{18}	72	91	0.134	27.0	27.0	29.4	1	20.3
Allure-C_{18}	230	291	0.335	26.7	23.8	23.0	0.89	21.3
Xterra-C_{18}	115	146	0.501	44.9	58.6	68.9	1.3	20.6
YMC-C_{18}	201	254	0.586	52.7	46.5	46.1	.88	20.6
Gemini-C_{18}	170	215	0.531	42.4	46.5	49.4	1.1	22.1
XBridge-C_{18}	120	152	0.471	74.7	69.7	62.0	0.93	21.7

Figure 3-1 Full nitrogen adsorption isotherms for all studied adsorbents.
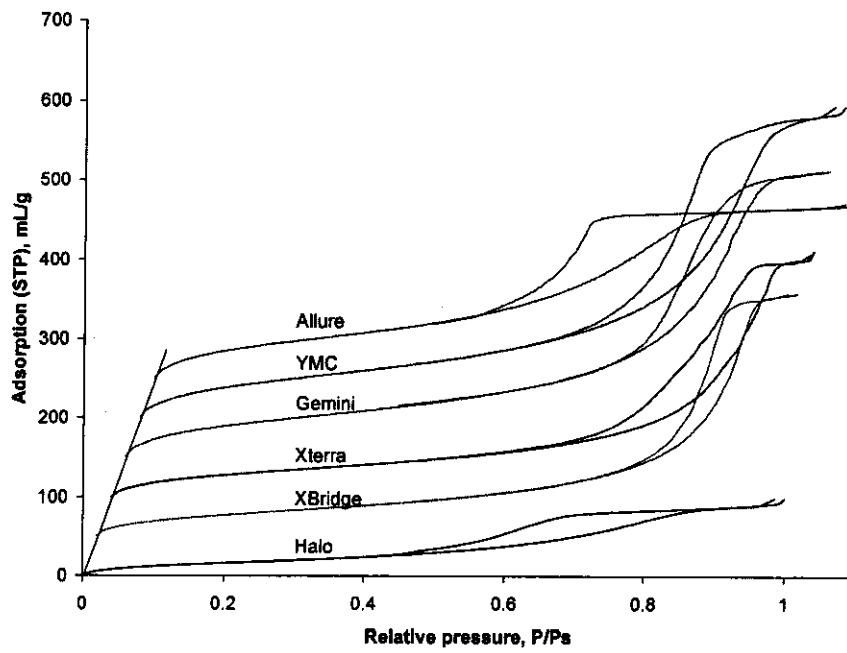
adsorbents made with the same base silica and when chemical surface modification did not

alter significantly the adsorbent geometry. B. Buszewski recently [112] suggested the use of a

cylindrical pore model for the determination of the actual surface area of modified adsorbents.

The cylindrical pore model assume the applicability of the following relationship between

pore volume, surface area and pore radius:

$$\frac{V_p}{S} = \frac{R}{2} \qquad\qquad 3\text{-}1$$

The ratio of the specific pore volume to the specific surface area should be equal to the half of

the pore radii. Modern HPLC adsorbents have significant pore size distribution, some

distributions are asymmetric. Pore radius determined from the maximum of the distribution

curve is significantly different from the median pore radius. In Figure 3-2, the pore size

distributions for studied adsorbents are shown. Columns 4 and 5 in the Table 3-2 show the

maximum and median values of the pore radius for studied adsorbents, and column 6

represents the pore radius calculated using eq. 3-1. As shown by these data, the median pore

radius values are closer to the values that are determined when the cylindrical pore model is

assumed, but the more asymmetric the pore size distribution the greater the difference

between these values.

The minimum relative standard deviation of the differences between the pore radii

calculated using the 2V/S relationship and the median pore radii obtained from the pore size

distribution is 35%. The Allure and YMC modified silicas show the best correlation with the

cylindrical pore model, even though their pore size distributions are not the most symmetric

ones. Interestingly, the Xterra and Xbridge adsorbents have the most asymmetric distributions

and also show the highest differences in calculated and measured pore radii. The most

symmetric pore size distributions are for the Halo and Gemini adsorbents. These significant

65

Figure 3-2   **Pore size distribution of studied adsorbents**
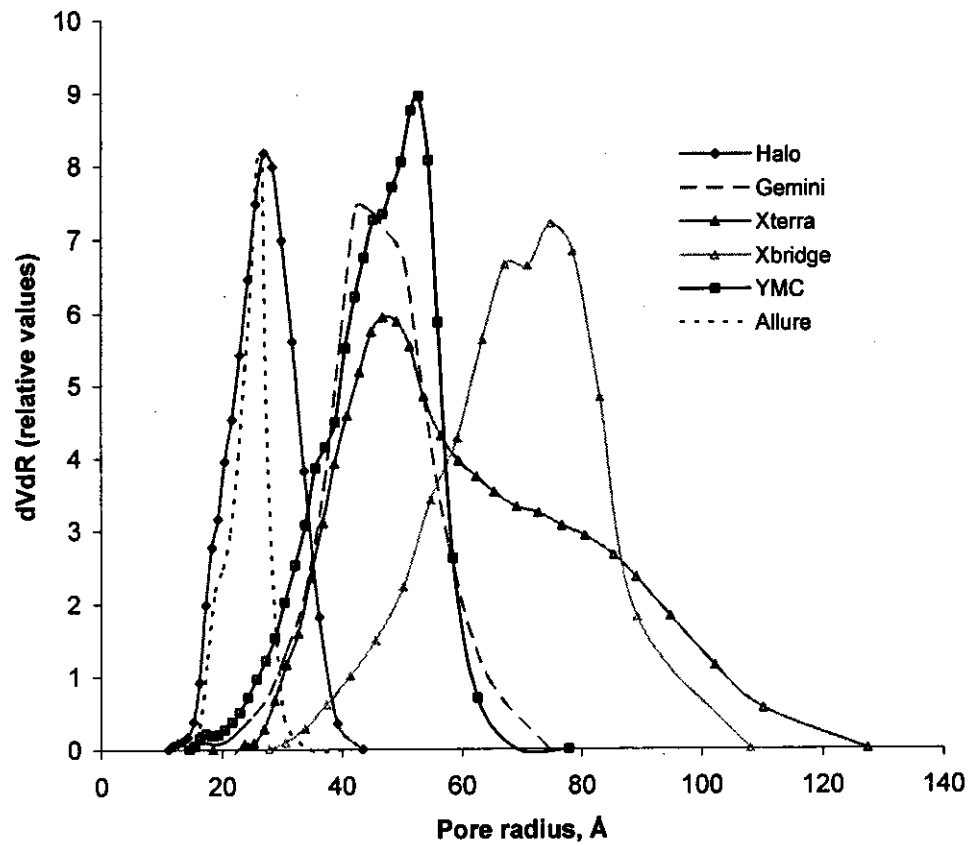
deviations from the cylindrical pore model may be due to the pore connectivity (networking effect) and indicate that it is better to avoid the use of the pore radius value in any adsorbent geometry calculations.

3.2   Column Characterization

The void volume of each column was measured by using the retention of deuterated MeOH eluted with pure MeOH, and the inter-particle volume was measured using an inverse GPC method. Experimental data (retention volumes) for V_{ip} determination by GPC using THF as mobile phase are shown in Table 3-3. Linear extrapolation of the retention dependence of polymer standards vs. cubic root of their molecular weight to zero molecular veight value in Figure 3-3 & Figure 3-4 which give sample independent value of inter-particle volume. Apparently packing densities of all columns are significantly different

Table 3-1 shows the chromatographic characterization data for all columns including the measured and calculated weight of packing material in each column. The mass of adsorbent in the column was calculated according to the procedure described in [22] and using eq. 1-1. The actual surface areas of each column were calculated using the determined mass of adsorbent in the column and the adsorbent surface area (corrected for the increased molecular area of nitrogen on a hydrophobic surface (20.5/16.2)) and are listed in the last column of Table 3-1. As one can see, there is a significant difference among these columns in the total surface available for interaction with analytes. The relative standard deviation (RSD) of the ratio between the column void volumes to the empty column volume is only 12% for all of the columns in this study, whereas the deviation of the ratio between the column surface area and the empty column volume is 30%. Significant variation in the total surface area available in a

Table 3-3   Retention volumes of polystyrene standards determined by GPC

System Volume Corrected Retention Volums using GPC (mL)	Polystyrene Standard (MW)				
	382100	410000	860000	994000	1850000
Halo-C_{18}	0.329	0.326	0.324	0.321	0.319
Allure-C_{18}	0.834	0.823	0.822	0.807	0.804
Xterra-C_{18}	0.385	0.383	0.379	0.375	0.365
YMC-C_{18}	0.308	0.305	0.304	0.300	0.296
Gemini-C_{18}	0.381	0.380	0.373	0.372	0.365
XBridge-C_{18}	0.372	0.369	0.364	0.361	0.357

Flow rate: 0.5 ml/min.

Figure 3-3   Decrease of retention volume due to the molecular size of polystyrene

standards on Halo-C_{18}, Allure-C_{18}, and Xterra-C_{18}.
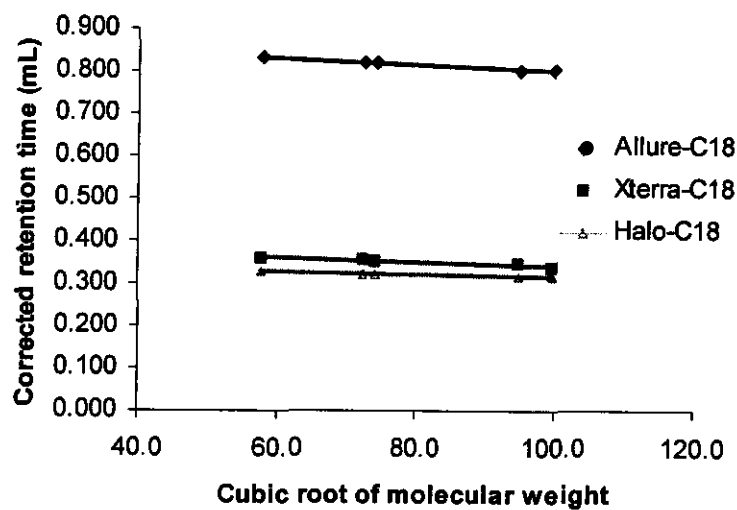
Figure 3-4   Decrease of retention volume due to the molecular size of polystyrene

standards on YMC-C_{18}, Gemini-C_{18} and XBridge-C_{18}.
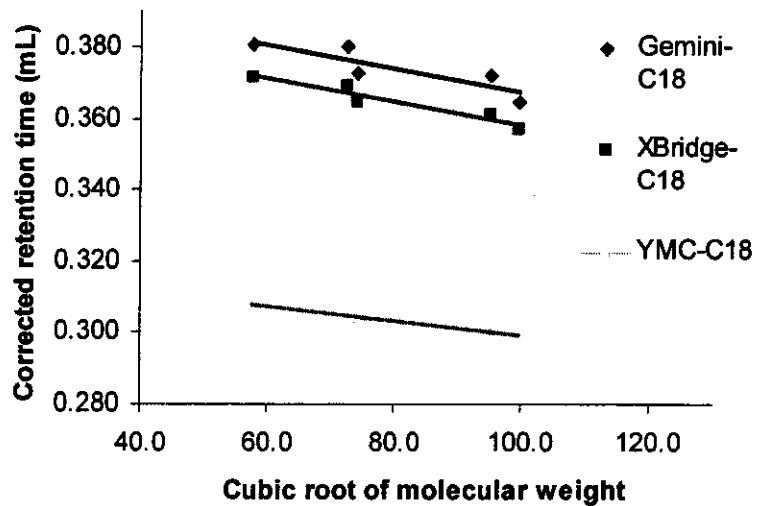
Table 3-4   Column geometry parameters

Adsorbent	V_o	V_{ip}	$m_{ads.}$ (measured)	$m_{ads.}$ (calc)	RSD%	S (total) (calc.)
	mL	mL	g	g		m^2
Halo-C_{18}	0.442	0.34	0.771	0.761	1.3	70
Allure-C_{18}	1.381	0.88	1.53	1.493	2.4	445
Xterra-C_{18}	0.740	0.40	0.681	0.677	0.5	99
YMC-C_{18}	0.595	0.32	0.461	0.464	0.7	117
Gemini-C_{18}	0.232	0.13	0.189	0.183	2.4	44
XBridge-C_{18}	0.71	0.41	0.652	0.645	0.7	99

column can be considered as an important factor in influencing the deviation of the retention of the same analyte on different columns that have the same surface chemistry.

To verify the influence of the adsorbent surface area on retention, V_R were determined and compared of three simple analytes, which were run on chromatographic systems that were purposely selected to avoid any secondary interactions. In this case, we determined the retention of benzene, toluene, and ethylbenzene on the columns in our study using two mobile phases; 70 MeCN/30 H_2O and 70 MeOH/30 H_2O. The retention volumes of benzene and the two alkylbenzenes are shown in Table 3-5 for all columns. In addition, the retention factors for the three analytes were then calculated and are shown in Table 3-6 together with the relative standard deviation for each analyte on all columns. The variation in retention factor is on the level of 35% for all of the analytes.

In 1970, Kiselev [53] described the chromatographic retention process on the basis of the theory of adsorption from solutions and argued for the use of surface-specific retention factors. In a more recent article, Kovats [36] introduced the "aerial retention volume" as the reduced retention volume related to the adsorbent surface area. He argued that this parameter represents the slope of the excess adsorption isotherm of an analyte at a given eluent composition and is a model-independent characteristic of analyte retention. We will designate this parameter as the "surface specific" retention factor, which essentially represents the fraction of the analyte retention associated with 1 square meter of the adsorbent surface. This parameter could be calculated as,

$$k_s = \frac{V_R - V_0}{S_{tot}}$$

3-2

Table 3-5   **Alkylbenzenes retention volumes (mL)**

Adsorbent	70/30 MeCN/H_2O			70/30 MeOH/H_2O		
	Benzene	Toluene	Ethylbenzene	Benzene	Toluene	Ethylbenzene
Halo-C_{18}	0.814	1.027	1.308	1.122	1.688	2.491
Allure-C_{18}	3.778	5.137	6.886	5.748	9.323	14.235
Xterra-C_{18}	1.250	1.5_{18}	1.863	1.796	2.5_{18}	3.543
YMC-C_{18}	1.238	1.579	2.025	1.658	2.507	3.695
Gemini-C_{18}	0.469	0.574	0.711	0.622	0.891	1.259
XBridge-C_{18}	1.254	1.551	1.938	1.674	2.415	3.44

Table 3-6   **Alkylbenzenes Retention factors**

Adsorbent	70/30 MeCN/H_2O			70/30 MeOH/H_2O		
	Benzene	Toluene	Ethylbenzene	Benzene	Toluene	Ethylbenzene
Halo-C_{18}	0.842	1.324	1.959	1.122	1.688	2.491
Allure-C_{18}	1.738	2.722	3.99	5.748	9.323	14.235
Xterra-C_{18}	0.689	1.051	1.5_{18}	1.796	2.5_{18}	3.543
YMC-C_{18}	1.081	1.654	2.403	1.658	2.507	3.695
Gemini-C_{18}	1.022	1.474	2.065	0.622	0.891	1.259
XBridge-C_{18}	0.766	$1._{18}5$	1.73	1.674	2.415	3.44
RSD%	*33.9*	*35.1*	*35.7*	*33.7*	*35.8*	*36.5*

where V_R is the analyte retention volume, V_0 is the column void volume, and S_{tot} is the total surface area of the adsorbent in the column. We would not argue that this parameter is model independent and immediately represent the analyte adsorption equilibrium, as stated by Kovats [36] since the studied chromatographic system is essentially a three-component system and the analyte adsorption isotherm is not a line but a surface. Thus, the slope of the isotherm is dependent on the mutual reaction of the analyte and organic modifier to the equilibrium disturbance introduced by the injection of the analyte. As it is also related to the proper measurement of the total adsorbent surface area, this parameter is undoubtedly better suited for the comparison of different columns with similar surface chemistry. The illustration of this statement is shown in Table 3-7, where the surface-specific retention factors are shown for all of the studied analytes. As one can see, the relative standard deviation of the retention parameters for the same analyte at the same conditions among different columns has decreased 9-10 times, which is clearly visible where retention factors (Figure 3-5) and surface-specific retention (Figure 3-6) graphically for each column.

Table 3-7   Alkylbenzenes Surface specific retention factors [uL/m^2]

Adsorbent	70/30 MeCN/H$_2$O			70/30 MeOH/H$_2$O		
	Benzene	Toluene	Ethylbenzene	Benzene	Toluene	Ethylbenzene
Halo-C$_{18}$	5.30	8.33	12.33	9.68	17.74	29.17
Allure-C$_{18}$	5.39	8.44	12.37	9.81	17.84	28.87
Xterra-C$_{18}$	5.15	7.86	11.35	10.67	17.97	28.33
YMC-C$_{18}$	5.48	8.39	12.20	9.07	16.31	26.44
Gemini-C$_{18}$	5.77	8.32	11.66	9.49	16.04	24.99
XBridge-C$_{18}$	5.51	8.52	12.44	9.77	17.28	27.66
RSD%	3.5	2.5	3.4	4.9	4.4	5.3

Figure 3-5   **Column-to-column variation of surface specific retention factors**
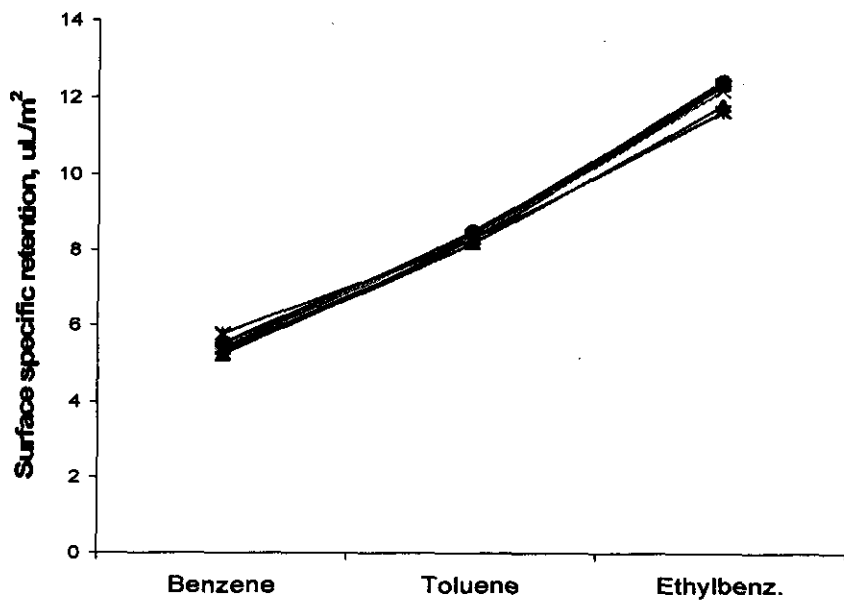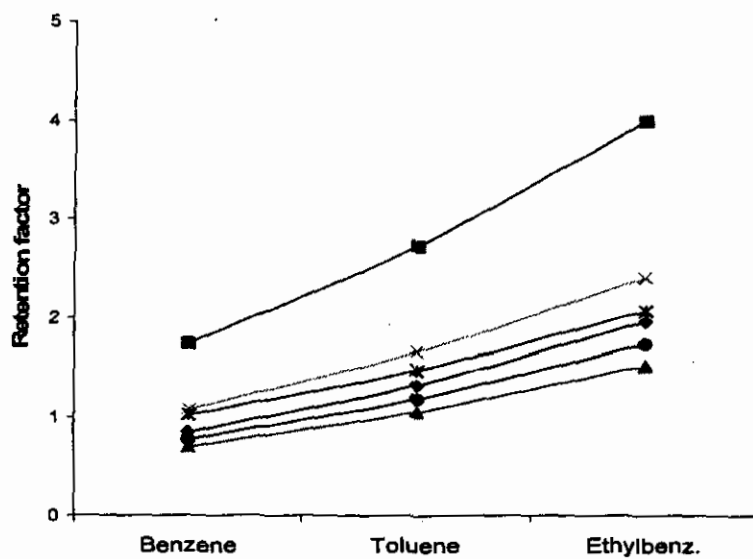
Figure 3-6   **Column-to-column variation of conventional retention factors.**

3.3 Bonding density evaluation

The authors of ref [112] also suggested use of the bonding density value for the calculation of the modified adsorbent surface area. Bonding density is a very important adsorbent characteristic because it indicates the degree of hydrophobicity of the corresponding packing material. However, this statement could be questionable for modern composite materials, such as Xterra, XBridge, and Gemini, since the base silica itself already contains alkyl moieties and thus it is less hydrophilic and accepts a lower degree of chemical modification. In addition, these composite materials also could not be analyzed by the end-user for verification of the carbon loading and bonding density parameters. Halo, Allure, and YMC materials are based on regular base silica, and TGA analysis in an air environment was used to obtain the weight loss and to collect a sufficient amount of base silica material for subsequent nitrogen adsorption analysis. The direct correlation of the TGA and CHN analyses was previously shown by Fadeev [121] for different types of ligands bonded on the surface of the silica.

It was shown previously that a bonded C_{18} ligand occupies ~600 $Å^3$ on the surface of silica [22], which is in good agreement with the molecular volume of eicosan (595 $Å^3$) that was calculated using ACDLabs (Toronto, Canada) software. (Eicosan (C20) is used because surface bonded alkylsilane C_{18} has two methyl side-groups with overall number of carbons equal to 20). These values could be used for the estimation of bonding density from the difference between the pore volumes of unmodified and modified adsorbent. The pore volume of the base silica minus the volume of bonded layer is equal to the pore volume of modified adsorbent per gram of base silica.

$$V_{p(SiO_2)} - v_{lig.} \cdot d_b \cdot S_{SiO_2} = \frac{V_{p(mod.)}}{f} \qquad 3\text{-}3$$

The conversion of the pore volume per gram of base silica to the measured specific pore volume of modified silica could be done using correction factor [22]:

$$f = \frac{1}{1 + d_b \cdot S_{SiO_2} MW_{lig}} \qquad 3\text{-}4$$

Where d_b is the bonding density, S is the surface of base silica, and $MW_{lig.}$ is the molecular weigh of bonded ligand. Solving these two equations for d_b we obtain

$$d_b = \frac{V_{p(SiO_2)} - V_{p(mod.)}}{S_{SiO_2}\left(v_{lig.} + V_{p(mod.)} \cdot MW_{lig.}\right)} \qquad 3\text{-}5$$

Another way to calculate bonding density is based on the weight loss values obtained from TGA experiments, and could be done with the following expression

$$d_b = \frac{w\%}{mw_{lig.} \cdot S_{SiO_2} \cdot (100 - w\%)} \qquad 3\text{-}6$$

where $w\%$ is the percent of weight loss, $m_{wlig.}$ is the weight of the cleaved portion of the ligand (283 g/mole), and S_{SiO2} is the surface area of silica.

80

In these calculations, it is assumed that all of the organic moieties were completely burned off into the air, while the silica atoms were left on the surface. All TGA experiments were performed by heating at 10 °C/min up to a final temperature of 550 °C. Subsequent BET analysis of the materials that remained after TGA showed C-constant values on the level of 50, which indicates a partial dehydroxylation of the silica surface. These calculations can be only considered as an estimate, since the degree of dehydroxylation is unknown, although it probably does not introduce a very significant error.

The characteristics of the packed materials that were provided by the manufacturers are shown in Table 3-8. In the last column of Table 3-8, the bonding density values that were calculated using the manufacturers' data are shown. For the Allure material, the surface area measured after TGA was used in the calculation, since manufacturer did not provide this information.

The adsorbent pore volume, measured surface area, and bonding density calculated using eqs 3-5 and 3-6 are shown in Table 3-9. As could be seen from comparison of the last two columns of Table 3-9, both methods gave consistent results. Bonding density values for Allure and YMC materials are also close to the values that were calculated from the manufacturer's data, while for the Halo material, the given value is much higher than the value calculated from the decreased pore volume and the TGA weight loss.

Table 3-8   **Manufacturers data on materials surface chemistry**

	Manufacturer's data			d_b (calc)
	S (base)	d_b	C%	
Halo-C_{18}	150	3.5	n.a	n.a
Allure-C_{18}	n.a.	n.a	27	3.6
YMC-C_{18}	334	n.a	15.9	2.5

Table 3-9   Comparison of the bonding density values calculated using different methods.

	Surface area	Pore volume (modified)	Pore volume (base silica)	Weight loss	d_b from pore volume	d_b (from weight loss)
	m^2/g	m^2/g	mL/g	w%	$\mu mol/m^2$	$\mu mol/m^2$
Halo-C_{18}	132	0.134	0.275	8	2.6	2.5
Allure-C_{18}	460	0.335	1.12	32	3.7	3.6
YMC-C_{18}	351	0.586	1.12	18	2.7	2.3

3.4   Adsorption behavior of eluent components

The void volume of the column (V_0) is obtained by integrating the plot of the retention times (V_R) of the perturbation peaks (from 0 to 100% of the organic modifier) [64]:

$$V_0 = \frac{\int_{c=0}^{c=max} V_R(c)\,dc}{c_{max}} \qquad 3\text{-}7$$

where c_{max} is a maximum concentration of the organic modifier in the mobile phase.

When c_{max} is known, the excess amount of the adsorbed organic modifier per unit amount of stationary phase (Γ) can be calculated [22]:

$$\Gamma_{(c)} = \frac{\int_{c=0}^{c=max} (V_R(c) - V(o))\,dc}{S} \qquad 3\text{-}8$$

where S is a total surface area of the stationary phase (m^2). In our experiments, the excess isotherm was calculated using the total surface areas in Table 3-4 for all six columns.

Experimental data of retention volumes by minor disturbance method in the binary eluent system with MeCN/H$_2$O and MeOH/H$_2$O on six columns at room temperature are summarized in Table 3-10 &Table 3-11, respectively. Retention profile of minor disturbance peaks of MeCN and MeOH are shown in Figure 3-7, Figure 3-8, Figure 3-8, and Figure 3-8. These dependencies were used for the calculation of the column void volumes shown in Table 3-12 using Eq. 3-7 and the excess adsorption isotherms using Eq. 3-8. The retention volume profiles versus the eluent composition for the same eluent on each column are quite similar, but the trend of changes is slightly different.

Table 3-10   Minor disturbance peak retention volumes in MeCN-H$_2$O binary system

MeCN Concentration (%, v/v)	System Volume Corrected Retention Volums (mL)					
	Halo-C$_{18}$	Allure-C$_{18}$	Xterra-C$_{18}$	YMC-C$_{18}$	Gemini-C$_{18}$	XBridge-C$_{18}$
0	0.624	2.529	1.933	1.086	0.354	1.093
1	0.579	2.155	1.211	0.888	0.311	1.002
5	0.537	1.974	0.943	0.754	0.273	0.861
10	0.520	1.899	0.835	0.707	0.259	0.801
20	0.495	1.786	0.776	0.666	0.252	0.764
30	0.461	1.471	0.734	0.610	0.233	0.728
40	0.420	1.178	0.670	0.537	0.205	0.668
50	0.392	1.028	0.607	0.475	0.$_{18}$3	0.598
60	0.378	0.973	0.560	0.442	0.168	0.548
70	0.380	0.971	0.553	0.437	0.165	0.541
80	0.391	1.015	0.581	0.457	0.172	0.568
90	0.409	1.117	0.620	0.493	0.$_{18}$5	0.604
95	0.425	1.213	0.646	0.541	0.197	0.633
99	0.454	1.339	0.707	0.619	0.213	0.677
100	0.480	1.400	0.794	0.680	0.222	0.751

Table 3-11   **Minor disturbance peak retention volumes in MeOH-H$_2$O binary system**

MeOH Concentration (%, v/v)	System Volume Corrected Retention Volums (mL)					
	Halo-C$_{18}$	Allure-C$_{18}$	Xterra-C$_{18}$	YMC-C$_{18}$	Gemini-C$_{18}$	XBridge-C$_{18}$
0	0.4765	1.602	0.956	0.734	0.259	0.945
1	0.4612	1.575	0.868	0.706	0.248	0.823
5	0.4524	1.528	0.777	0.640	0.232	0.767
10	0.4456	1.481	0.726	0.601	0.222	0.738
20	0.435	1.377	0.685	0.566	0.212	0.711
30	0.4275	1.325	0.667	0.550	0.206	0.699
40	0.423	1.293	0.658	0.540	0.202	0.693
50	0.4202	1.271	0.652	0.534	0.200	0.689
60	0.4$_{18}$7	1.261	0.653	0.533	0.199	0.686
70	0.4191	1.258	0.652	0.534	0.199	0.684
80	0.4205	1.270	0.659	0.541	0.201	0.684
90	0.4235	1.286	0.671	0.549	0.206	0.686
95	0.4265	1.294	0.677	0.556	0.211	0.702
99	0.4305	1.305	0.683	0.578	0.217	0.762
100	0.4345	1.315	0.694	0.643	0.220	0.826

Figure 3-7 Dependencies of the minor disturbance peaks retention volumes for

$MeCN:H_2O$ on Halo-C_{18}, Allure-C_{18} and Xterra C_{18}.

Retention Volume (mL)

MeCN Eluent Composition (% v/v)

△—△ Halo-C18
◆—◆ Allure-C18
⊖—⊖ Xterra C18
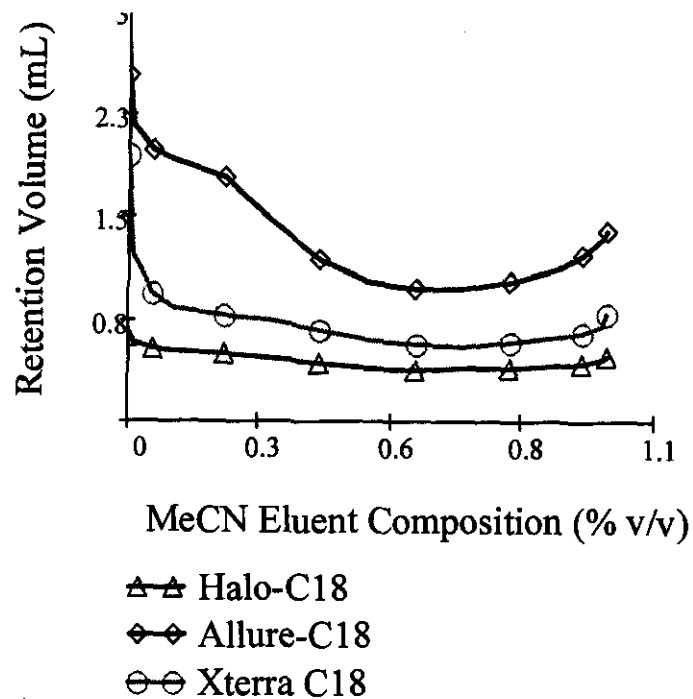
Figure 3-8   Dependencies of the minor disturbance peaks retention volumes for

MeCN:H_2O on YMC-C_{18}, Gemini-C_{18} and XBridge-C_{18}.

△—△ YMC-C18
◇—◇ Gemini-C18
⊖—⊖ XBridge-C18
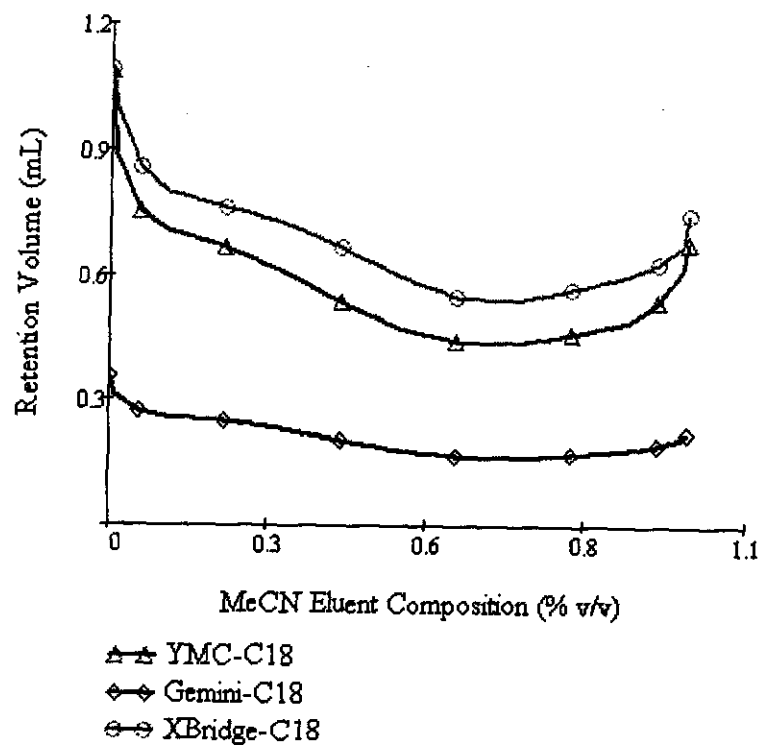
Figure 3-9 Dependencies of the minor disturbance peaks retention volumes

for MeOH : H_2O on Halo-C_{18}, Allure-C_{18} and Xterra C_{18}.
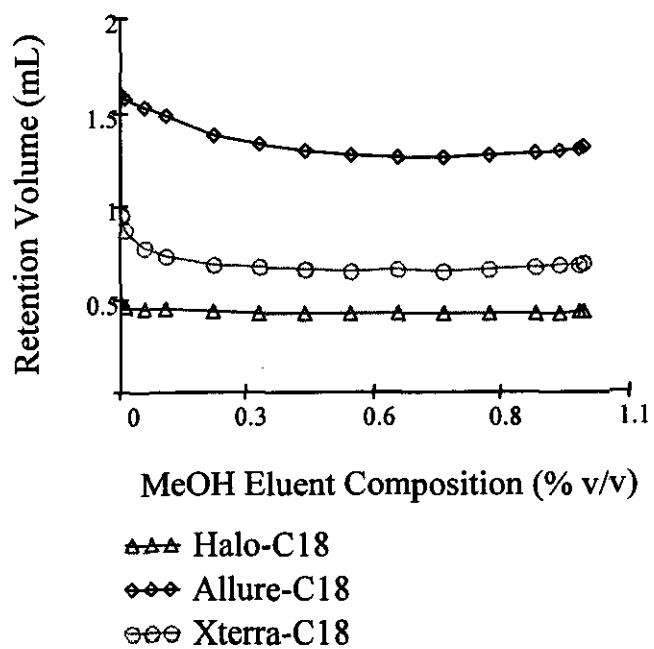
Figure 3-10 Dependencies of the minor disturbance peaks retention volumes for MeOH :H₂O on YMC-C₁₈, Gemini-C₁₈ and XBridge-C₁₈.

△—△ YMC-C18
◆—◆ Gemini-C18
⊖—⊖ XBridge-C18
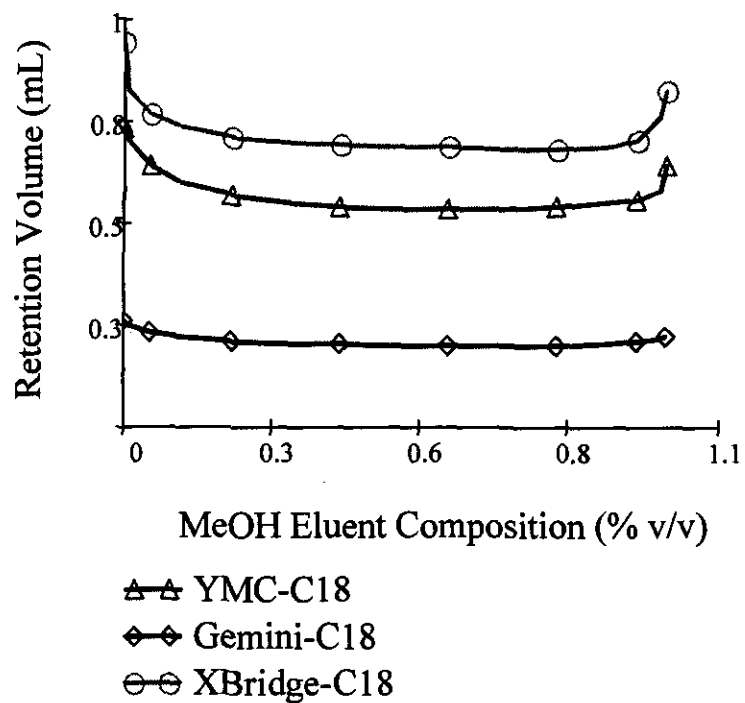
Table 3-12   **Void volumes measured with MeCN-H$_2$O and MeOH-H$_2$O binary system by minor disturbance method**

Adsorbent	V_o (MeCN) (mL)	V_0 (MeOH) (mL)
Halo-C$_{18}$	0.436	0.428
Allure-C$_{18}$	1.319	0.1.327
Xterra-C$_{18}$	0.691	0.680
YMC-C$_{18}$	0.557	0.559
Gemini-C$_{18}$	0.208	0.208
XBridge-C$_{18}$	0.665	0.706

3.4.1 Adsorption of MeOH and MeCN from H_2O

The overlay of the excess adsorption isotherms of the same component (MeCN & MeOH) on different surfaces reveals the heterogeneity of the C_{18} determined silica surface. Figure 3-11and Figure 3-12 represent the calculated excess isotherms of MeCN, while Figure 3-13 and Figure 3-14 shows the excess isotherms of MeOH. The profile of the excess adsorption isotherm shows an increase of the adsorbate accumulation on the surface up to approximately 30~40% (v/v) of the adsorbate in the equilibrium solution. At 30~40% (v/v), the maximum of the excess amount adsorbed is observed. Further increase of the equilibrium concentration leads to the steady decrease of the excessive adsorbed quanity until it reaches a zero value at 100% (v/v) of the adsorbate in the bulk liquid. It is known that the adsorption of MeCN on hydrophobic stationary phase is much stronger than the adsorption of MeOH [26]. Therefore, the linear region of the isotherm and the maximum of the isotherm are higher for MeCN. This result agrees well with the data presented by Kazakevich at. [44]. The location of the maximum of the excess isotherm for MeCN is shifted towards higher concentration of the organic modifier than in the case of MeOH. This behavior is observed for all tested stationary phases.

Figure 3-15 and Figure 3-16 shows the magnified MeCN-rich and MeOH-rich region of excess adsorption isotherm. In Figure 3-15, the shape of most curves for the excess isotherms of MeCN on all tested stationary phases is similar. Every isotherm except Allure-C_{18}'s has a small negative part for high concentration of MeCN in the mobile phase. This phenomenon is caused by the adsorption of H_2O. Allure-C_{18} has zero negative excess in the curve. In Figure 3-16, most of the curves also show a similar manner with a negative excess

Figure 3-11 **Excess adsorption isotherm of MeCN from H_2O on Halo-C_{18}, Allure-C_{18}, and Xterra-C_{18}**
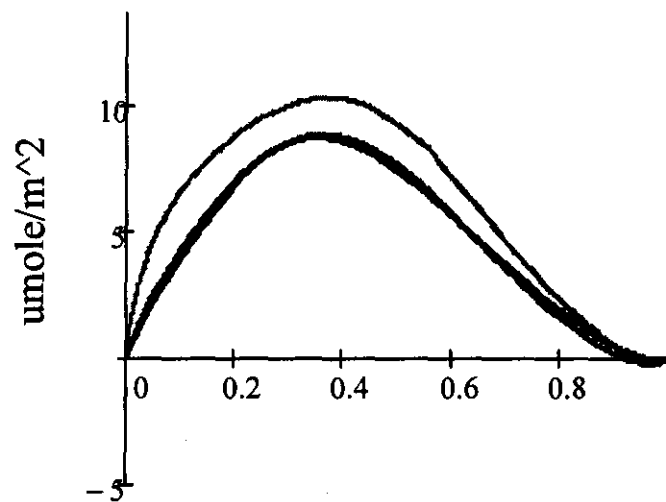
MeCN Eluent Composition (%v/v)

— Halo-C18
— Allure-C18
— Xterra-C18

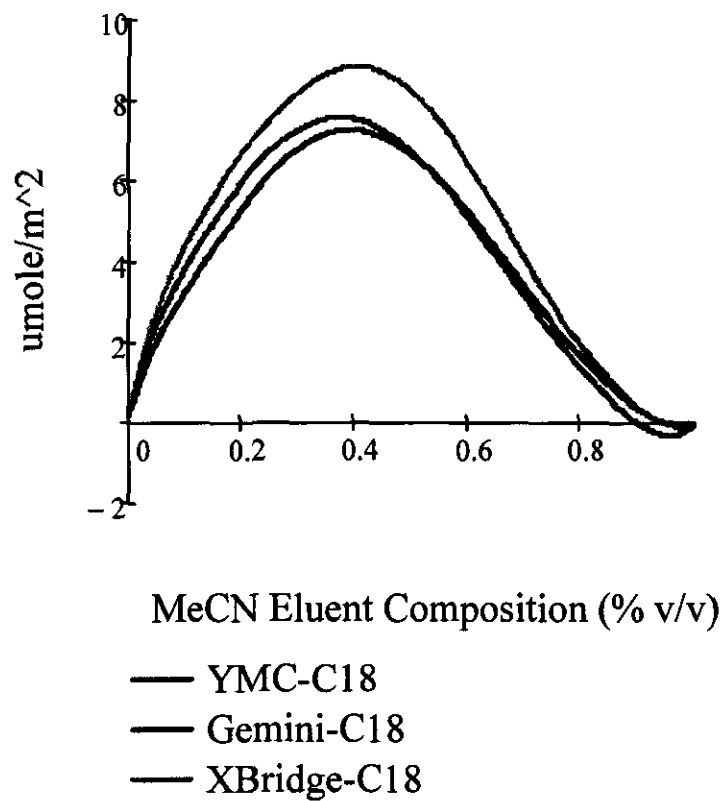**Figure 3-12**   Excess adsorption isotherm of MeCN from H_2O on YMC-C_{18}, Gemini-

C_{18}, and XBridge-C_{18}

MeCN Eluent Composition (% v/v)

—— YMC-C18
—— Gemini-C18
—— XBridge-C18

Figure 3-13   Excess adsorption isotherm of MeOH from H_2O on Halo-C_{18}, Allure-C_{18}, and Xterra-C_{18}

MeOH Eluent Composition (% v/v)

—— Halo-C18
—— Allure-C18
—— Xterra-C18
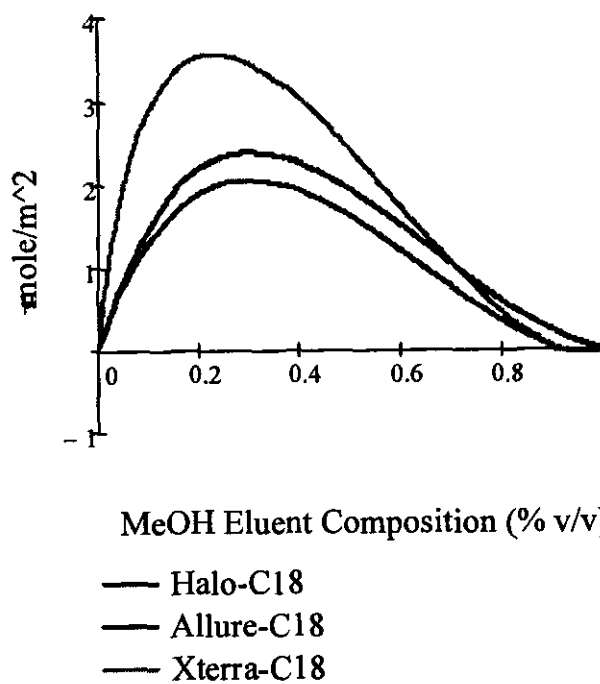
Figure 3-14   **Excess adsorption isotherm of MeOH from H_2O on YMC-C_{18}, Gemini-C_{18}, and XBridge-C_{18}**

MeOH Eluent Composition (% v/v)

—— YMC-C18
—— Gemini-C18
—— XBridge-C18
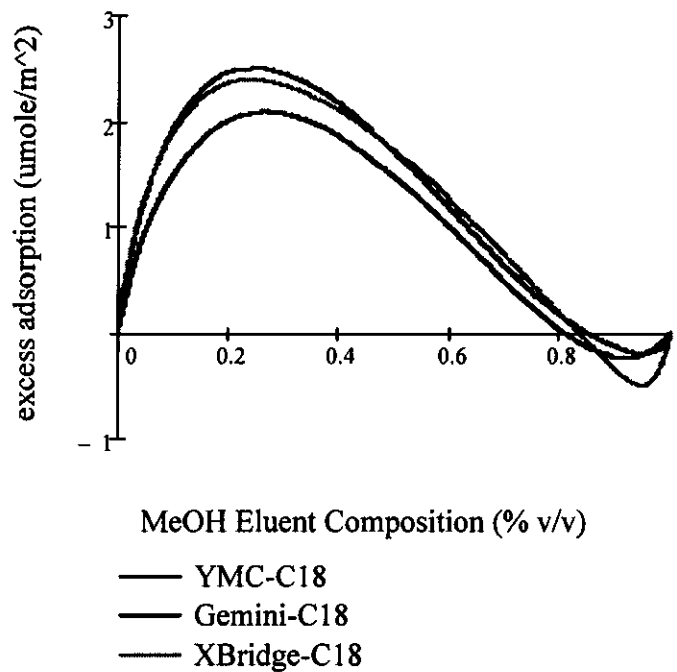
Figure 3-15   Magnified MeCN-rich region of excess adsorption isotherm
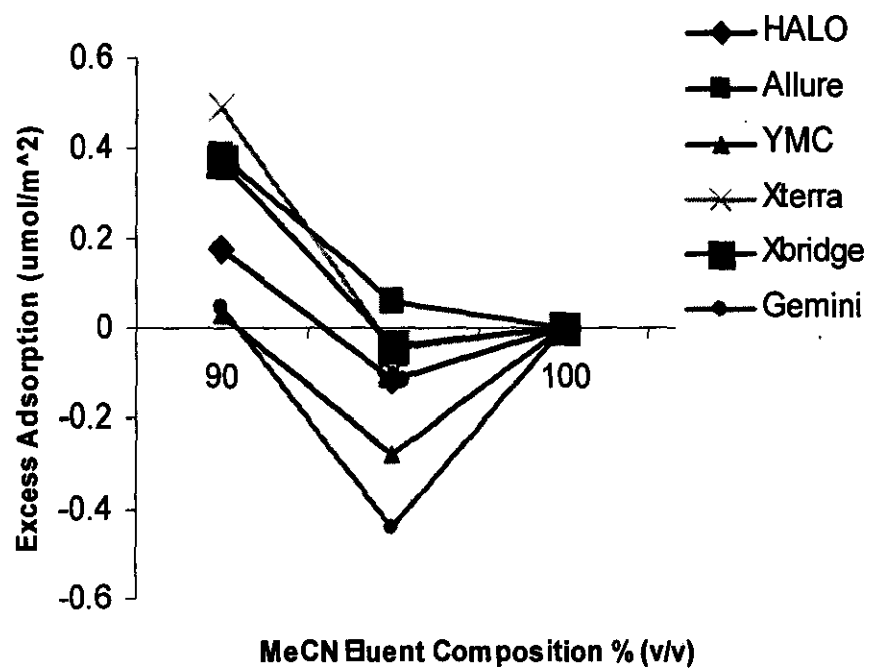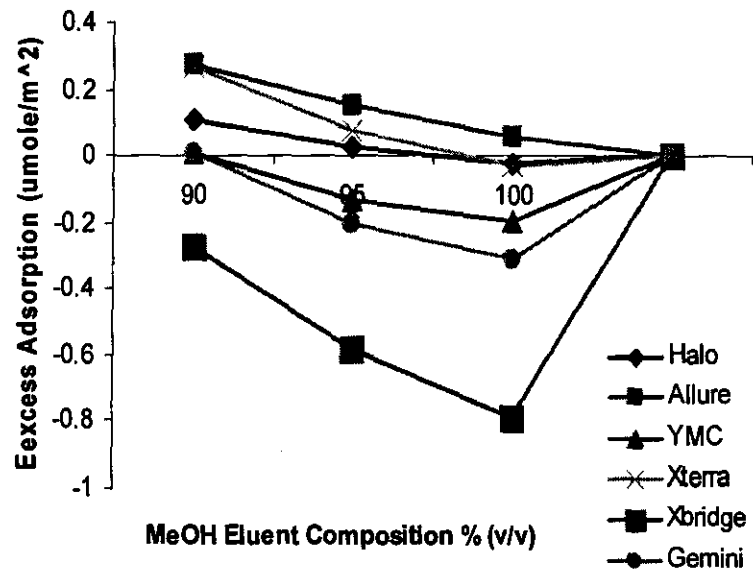
Figure 3-16   Magnified MeOH-rich region of excess adsorption isotherm

near the maximum % (v/v) of adsorbate in the equilibrium solution, which again indicates that the preferential adsorption of H_2O is observed. H_2O can adsorb on the residual silanols and other polar groups when they are present in the structure of the stationary phase [122]. The excess adsorption of MeOH on Allure-C_{18} stationary phase show relatively small negative excess. This indicates that the preferential type of the interaction for this column is hydrophobic. Allure-C_{18} is a special phase dedicated for separating polar analytes, including polar acidic compounds.

Compared to MeCN, significant amount of MeOH may be adsorbed near the silica surface through the hydrogen bonding with accessible residual silanols. Hydrogen-bonding may also form between H_2O and MeOH molecules. MeCN cannot interact with residual solanols which are exposed and H_2O molecules can adsorb on them. This explains why the excess adsorption isotherm of MeCN has more negative excess than that of MeOH.

The mole fraction of organic modifier x was calculated as follows:

$$x_i = \frac{\dfrac{c_i d_m}{M_m}}{\dfrac{c_i d_m}{M_m} + (100 - ci)\dfrac{d_w}{M_w}} \qquad 3\text{-}9$$

where c_i is the mobile phase equilibrium concentration (v/v), d_m and d_w are the densities of the organic modifier and H_2O, respectively, and M_m and M_w their molar mass.

A nonlinear relationship between the volume fraction (c) and mole fraction (x) of the mobile phase composition is illustrated in Figure 3-17.The comparison of the excess adsorption on the volume fraction versus the mole fraction is shown in Figure 3-18, Figure 3-19, Figure 3-20, Figure 3-21, Figure 3-22, Figure 3-23, Figure 3-24, Figure 3-25, Figure 3-26, Figure 3-27, Figure 3-28, and Figure 3-29 for all six columns in the MeCN-H_2O and MeOH-H_2O

binary system. Since the excess adsorption was measured using a model with a finite thickness layer on the surface [28], the volume fraction will better represent the adsorption behavior compared to the mole fraction by Guiochon [4].

The concentration of the adsorbate can be found by extrapolating the slope of the excess isotherm in a linear region to the y-axis or it can be calculated as the intercept parameter of the straight line fitted to the linear region of the excess isotherm (Figure 3-30). The thickness of the adsorbed layer (τ) can be calculated with the following equation [2]:

$$\tau = -\frac{Va}{S} = \frac{d\Gamma(c_e)}{Sdc_e} \qquad\qquad 3\text{-}10$$

The adsorption isotherm of the organic modifier can be calculated as the sum of the excess isotherm and the product of the thickness of the adsorption layer and the concentration in the mobile phase [2]:

$$n_{ads} = C\tau + \Gamma(c) \qquad\qquad 3\text{-}11$$

In Figure 3-31, Figure 3-32, Figure 3-33, and Figure 3-34, the full adsorption isotherms of the six columns on the component MeCN and MeOH versus the mole fraction (x) are shown. The organic layer thickness can be obtained from the platform in the adsorption isotherm. The calculated adsorbed layer thickness of MeOH and MeCN and H_2O fraction in these two binary systems was summarized in Table 3-13. MeOH's adsorption is approximately five times lower than MeCN. This is essentially consistent with the same behavior observed previously for adsorption on alkyl-modified adsorbents[22]. The adsorption of MeOH is predominantly monomolecular, while MeCN is adsorbed in multilayer fashion.

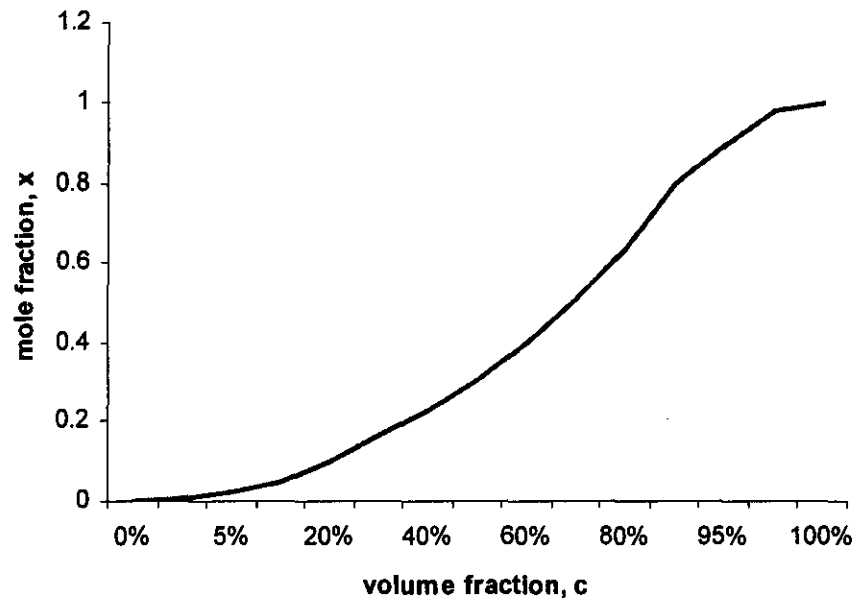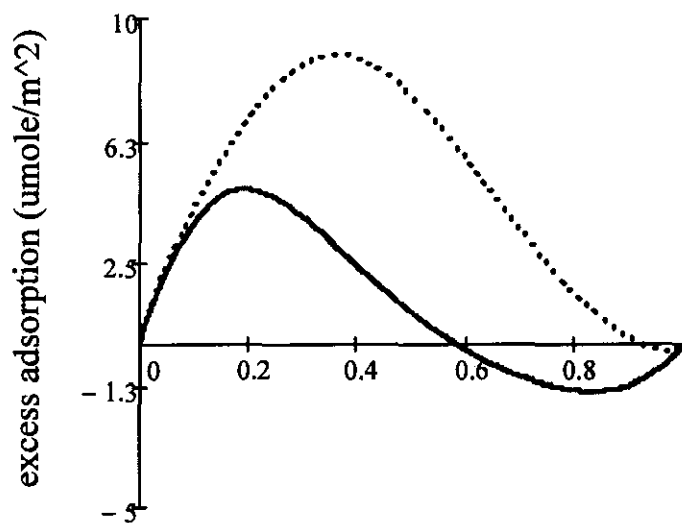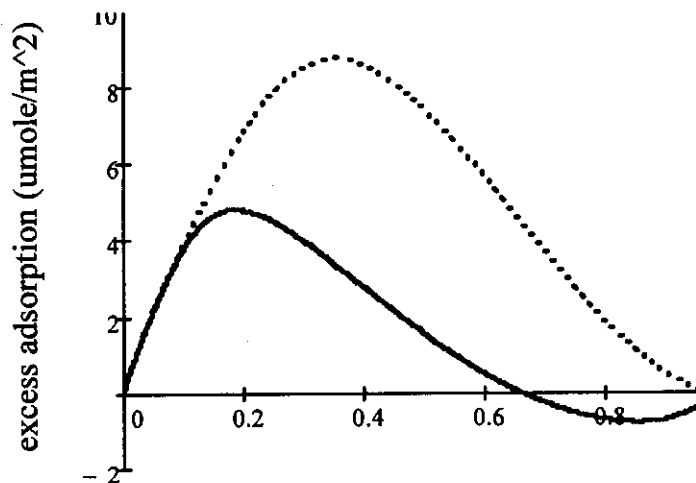**Figure 3-17**   Volume fraction (*f*) versus mole fraction (*x*) of

mobile phase composition

Figure 3-18   **Comparison of excess adsorption on volume fraction versus mole fraction (Halo-C_{18})**

Halo-C18 in aceonitrile/water system

—— Mole fraction
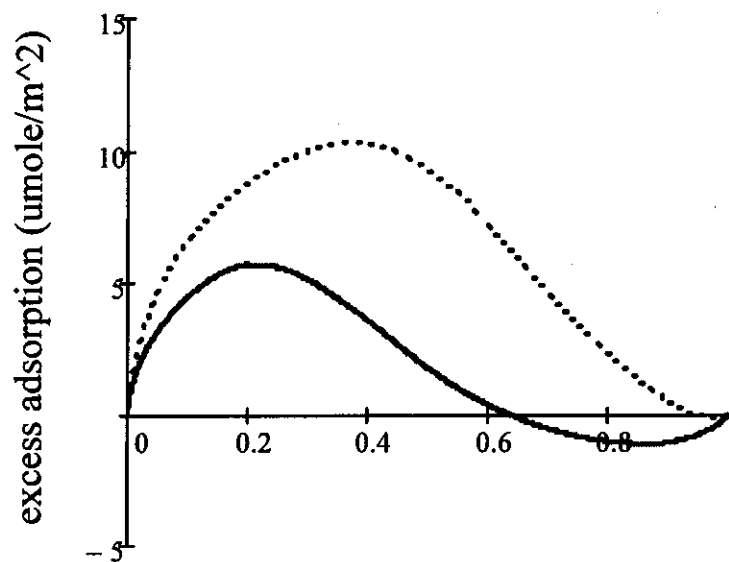····· Volume fraction

Figure 3-19   Comparison of excess adsorption on volume fraction versus mole

fraction (Allure-C_{18} with MeCN/H_2O binary system)

Allure-C18 in aceonitrile/water system

—— mole fraction

····· volume fraction

Xterra-C18 in aceonitrile/water system

——— volume fraction

····· mole fraction

Figure 3-21 Comparison of excess adsorption on volume fraction versus mole fraction (YMC-C_{18} with MeCN/H_2O binary system)
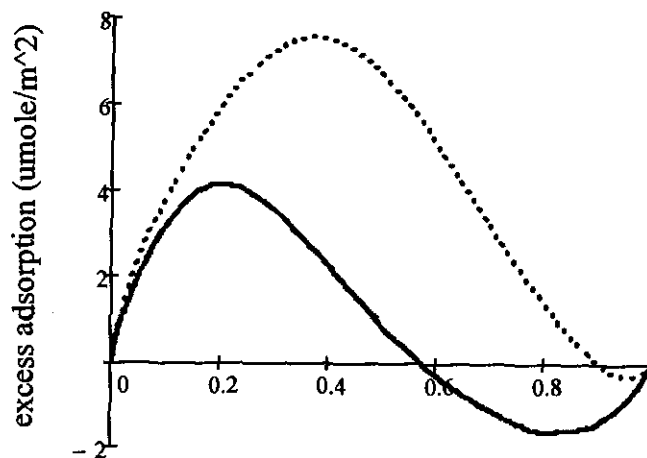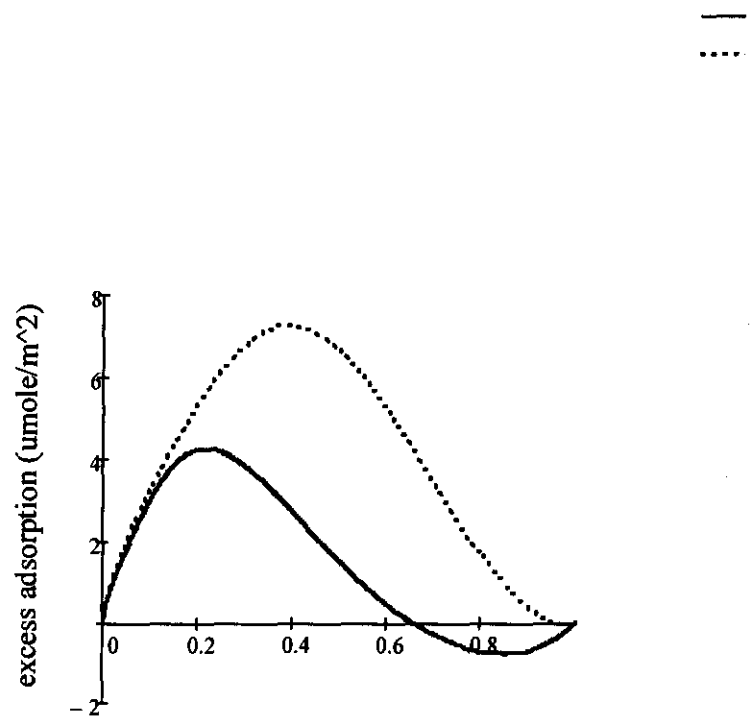

YMC-C18 in aceonitrile/water system

—— mole fraction

····· volume fraction

Figure 3-22   **Comparison of excess adsorption on volume fraction versus mole fraction (Gemini-C_{18} with MeCN/H_2O binary system)**

Gemini-C18 in aceonitrile/water system
—— mole fraction
····· volume fraction

Figure 3-23   Comparison of excess adsorption on volume fraction versus mole
fraction (Xbridge-C_{18} with MeCN/H_2O binary system)

XBridge-C18 in aceonitrile/water system

—— mole fraction
····· volume fraction

Figure 3-24 **Comparison of excess adsorption on volume fraction versus mole fraction (Halo-C_{18} with MeOH/H_2O binary system)**

Halo-C18 in methanol/water system

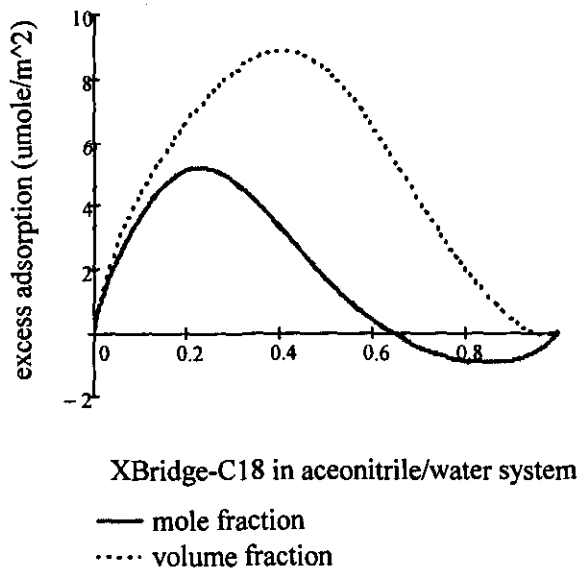— mole fraction

····· volume fraction

Figure 3-25 Comparison of excess adsorption on volume fraction versus mole

fraction (Allure-C_{18} with MeOH/H_2O binary system)

Allure-C18 in methanol/water system

—— mole fraction

····· volume fraction

Figure 3-26   Comparison of excess adsorption on volume fraction versus mole fraction (Xterra-C_{18} with MeOH/H_2O binary system)

Xterra-C18 in methanol/water system
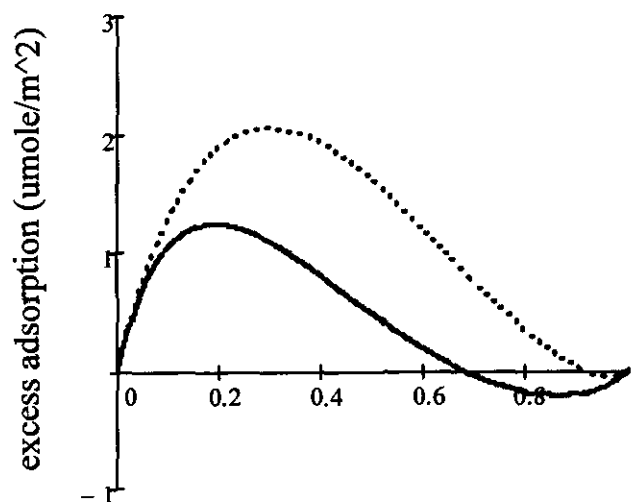
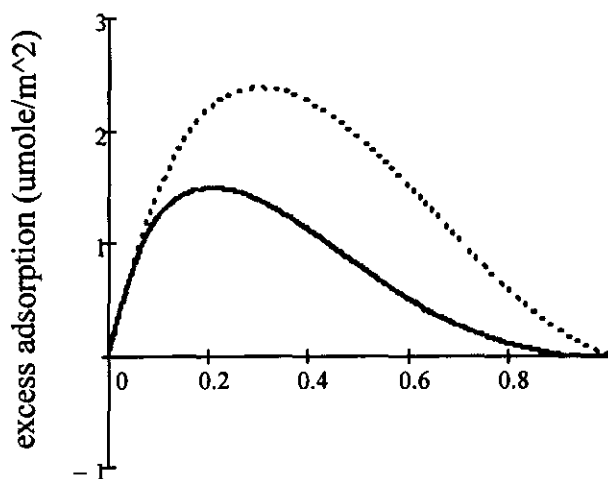—— mole fraction

····· volume fraction

Figure 3-27   Comparison of excess adsorption on volume fraction versus mole fraction (YMC-C$_{18}$ with MeOH/H$_2$O binary system)

YMC-C18 in methanol/water system

——— mole fraction
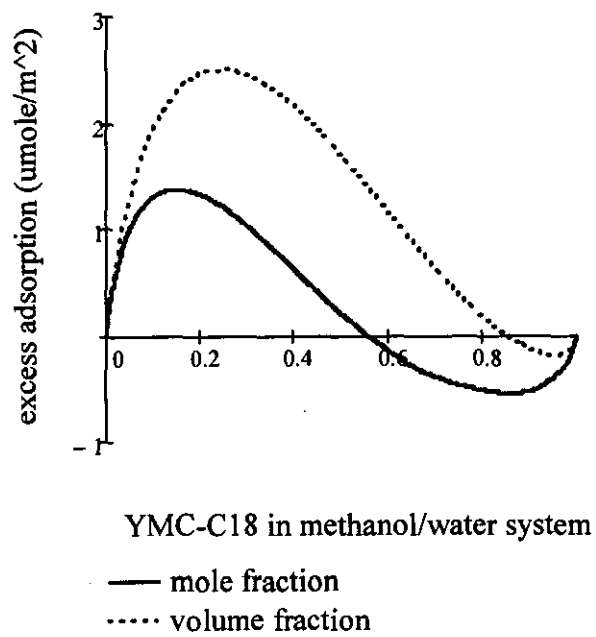
····· volume fraction

Figure 3-28   Comparison of excess adsorption on volume fraction versus mole fraction (Gemini-C_{18} with MeOH/H_2O binary system)

Gemini-C18 in methanol/water system

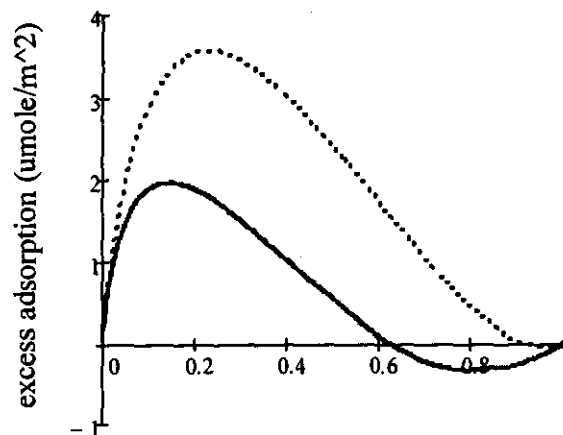—— mole fraction
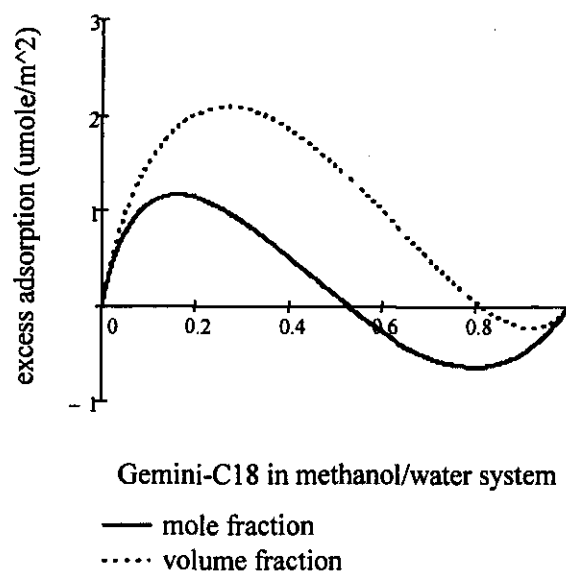
····· volume fraction

Figure 3-29   Comparison of excess adsorption on volume fraction versus mole

fraction (XBridge-C$_{18}$ with MeOH/H$_2$O binary system)
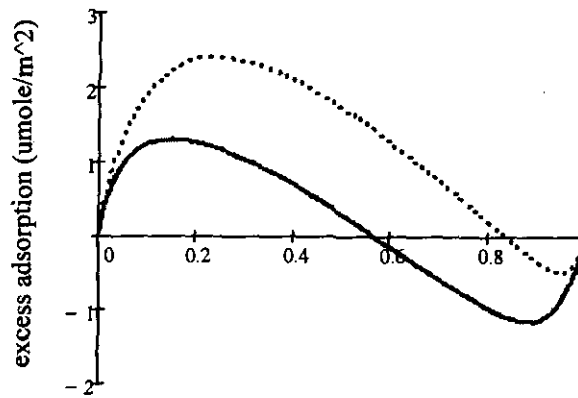
XBridge-C18 in methanol/water system

—— mole fraction

····· volume fraction

Figure 3-30   Determination of the amount of adsorbed organic eluent component.

The extrapolated y-intercept of the tangent ($c_r = 0$) to the downward slope of the isotherm (a_{max}) indicates the complete filling of the adsorbed layer where the total mount of organic adsorbed is constant.
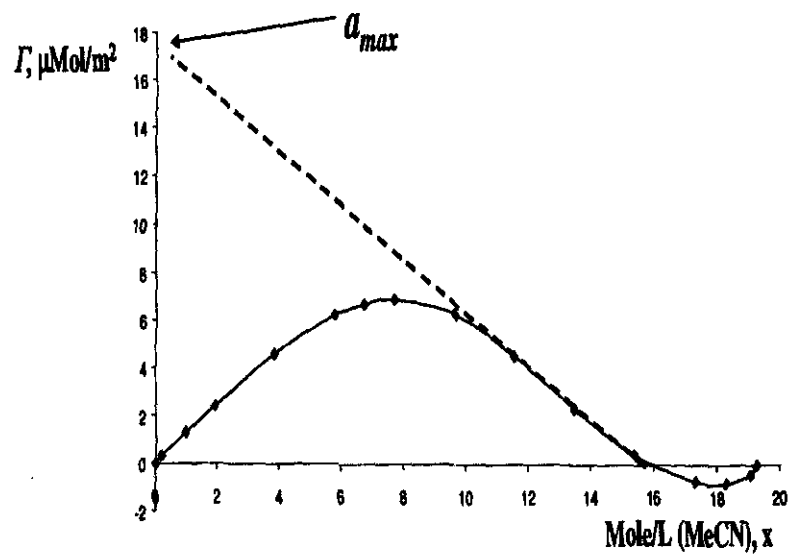
Figure 3-31   Full adsorption isotherm of MeCN from H_2O on Halo-C_{18}, Allure-C_{18}, and Xterra-C_{18}
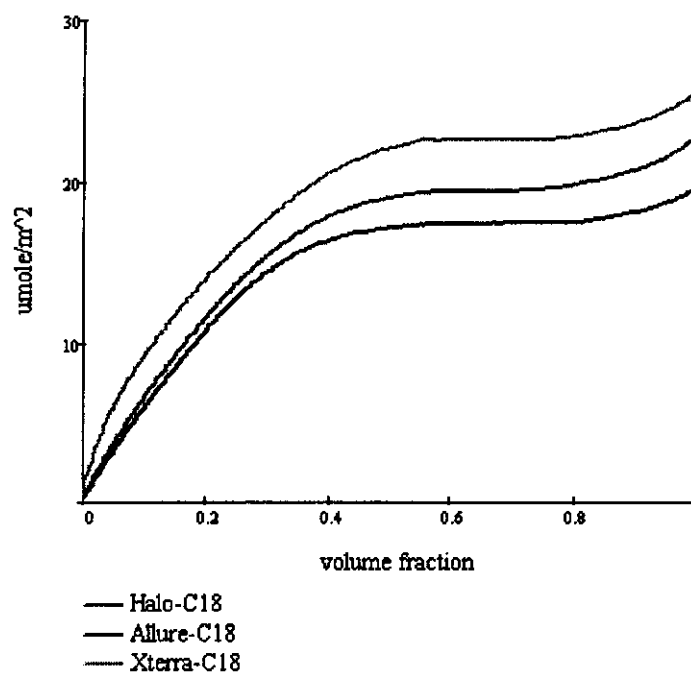
Figure 3-32   Full adsorption isotherm of MeCN from H_2O on YMC-C_{18}, Gemini-C_{18}, and XBridge-C_{18}

Legend:
— YMC-C18
— Gemini-C18
— XBridge-C18
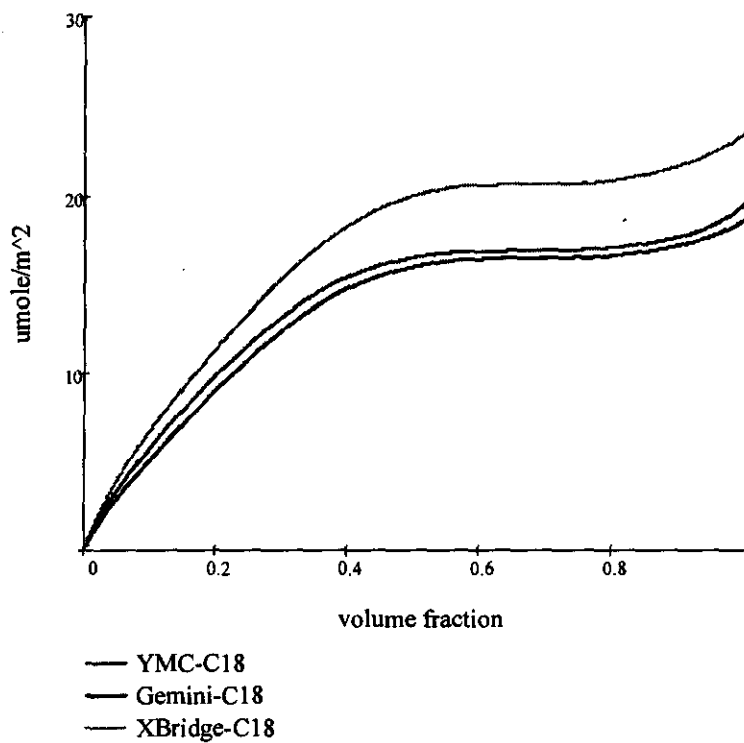
Figure 3-33   Full adsorption isotherm of MeOH from H_2O on Halo-C_{18}, Allure-C_{18},

and Xterra-C_{18}
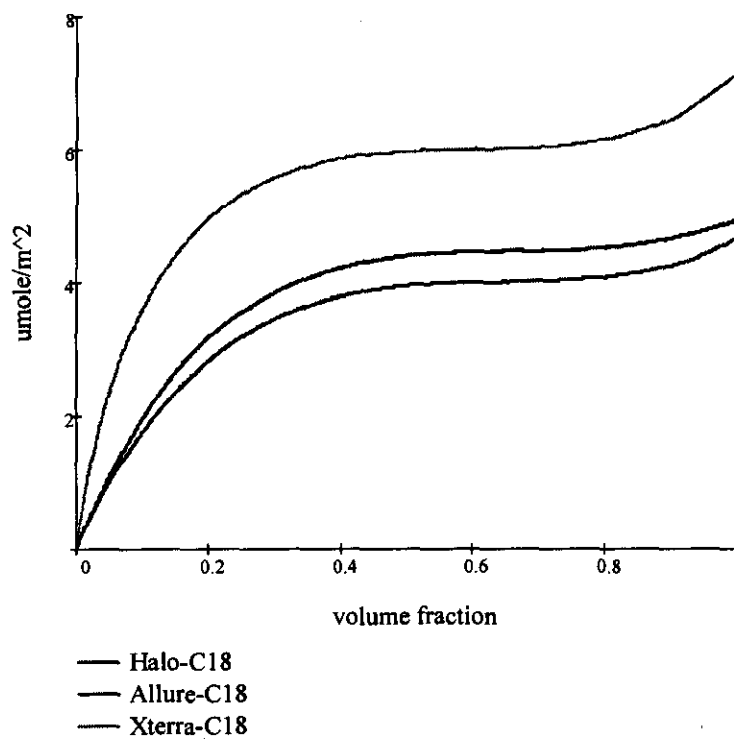
Figure 3-34   **Full adsorption isotherm of MeOH from H_2O on YMC-C_{18}, Gemini-C_{18}, and XBridge-C_{18}**

volume fraction

—— YMC-C18
—— Gemini-C18
········ XBridge-C18
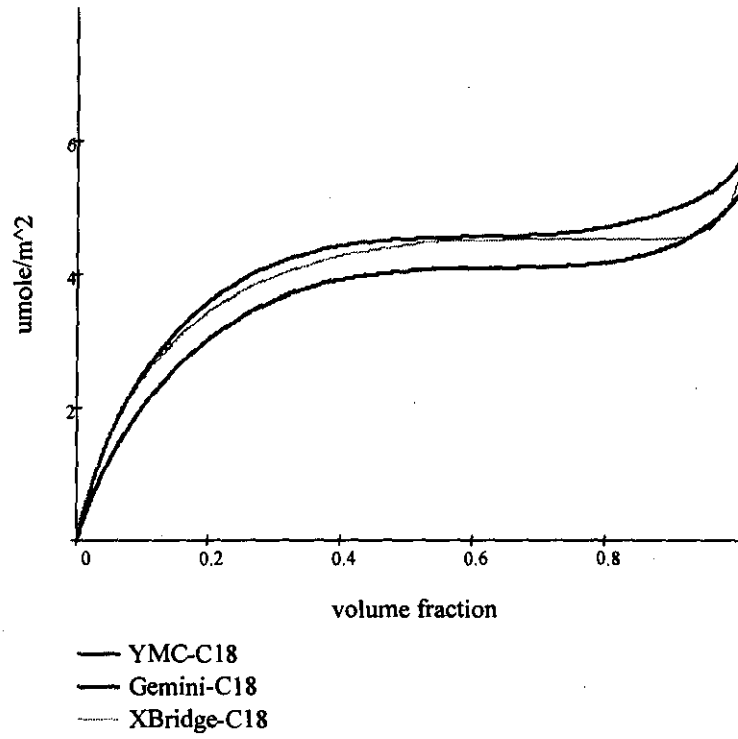
Table 3-13   Organic layer thickness on bonded phases

Adorbent	MeCN layer thickness (nm)	MeOH layer thickness (nm)
Halo-C_{18}	0.935	$0._{18}3$
Allure-C_{18}	1.004	0.193
Xterra-C_{18}	1.027	0.195
YMC-C_{18}	0.994	$0._{18}4$
Gemini-C_{18}	0.961	0.160
Xbridge-C_{18}	1.027	0.148

3.4.2   Surface heterogeneity

In RPLC, the mobile phase composition is different in the bulk mobile phase related to the surface of the adsorbent, which is characterized by the excess adsorbed amount of the organic modifier. In the structure of bonded phase of RPLC system, two types of adsorption centers are included: hydrophobic organic bonded ligands and hydrophilic residual silanols. Since excess adsorption isotherm is influenced by both the hydrophobic (organic modifier) and hydrophilic behavior (H_2O), it may provide a quantitative measurement of the heterogeneity of the adsorbent surface. Basically, this is based on an assumption that the adsorbent surface of RPLC columns is composed of two distinct patches: one represents the hydrophobic surface covered by the alkyl groups, the other is the polar and hydrophilic surface with the remaining accessible unreacted silanols after the surface derivatization.

All the full adsorption isotherms in Figure 3-31, Figure 3-32, Figure 3-33, and Figure 3-34 show that, at approximately 0.5 of mole fraction of organic modifier in the bulk solution, the formation of adsorbed layer is practically complete and there is no significant changes in the adsorbed layer volume until mole fraction greater than 0.9. Between 0.9 and 1 of the adsorbate in the bulk solution, the slight increase of the total adsorption isotherm is observed. We associate this with the displacement of H_2O observed on strong adsorption sites, which are the accessible residual silanols. The H_2O mole fraction was calculated using the full adsorption isotherms and the layer thickness:

$$w = \frac{a(1) - a(0.65)}{\dfrac{d_m}{M_m}\tau} \qquad\qquad 3\text{-}12$$

where $a(1)$ and $a(0.65)$ is the number of moles per square meter with the mole fraction of the organic modifier 1 and 0.65 respectively.

The calculated H_2O mole fraction of MeOH and MeCN and H_2O fraction in these two binary systems was listed in Table 3-14. For MeCN/H_2O sytem, Halo-C_{18} shows the highest value, and it has the highest negative excess adsorption; while Allure-C_{18} has the lowest value, and it has the lowest negative excess adsorption for the H_2O. For MeOH/H_2O system, Allure-C_{18} has the lowest value, which indicates that Allure-C_{18} has the least accessible residual sinlanoles. This is consistent with the highest value of bonding density for Allure-C_{18} in Table 3-9.

As discussed above, the difference between $a(1)$ and $a(0.65)$ tells how many moles of H2O are adsorbed on the residual silanols of the silica surface, defined as a_w. A linearity was elaborated by plotting a_w as a function of the bonding density d_B from Table 3-9 of the three adsorbents, Halo-C_{18}, Allure-C_{18}, and YMC-C_{18}, which is shown in Figure 3-35. The 2nd and 3rd column in Table 3-15 list the adsorbed H_2O amount per square meter from MeCN/H_2O and MeOH/H_2O binary systems, respectively.

By extrapolating to y-axis where d_B equals to 0, the resulting intercept can be thought of as the adsorbed H_2O amount per square meter for "zero bonding density", i.e.: a bare silica surface without modification. For MeCN/H_2O system, the intercept is 5.5 umol/m^2. This is in reasonable agreement with the value of adsorbed H_2O reported by Kondo, who found that the presence of the first layer of H_2O on the surface of bare silica is about 5.0 umol/m^2 based on FTIR measurements [123]. On the other hand, MeOH gives much lower value of the adsorbed H_2O amount. The intercept is only 1.9 umol/m^2 in MeOH/H_2O system. This can be rationalized based on the superior H-bonding capability of MeOH compared to MeCN. MeOH can act as both H-bonding donor and acceptor, meaning it is more competitive to H_2O compared to MeCN, which is only a H-bonding acceptor. A more systematic study could be

further approached for comparison of various RPLC adsorbents, which can differ over a wider

bonding density range.

Table 3-14   H₂O mole fraction adsorbed on bonded phases

Adsorbent	Hydrophilic surface fraction (MeCN)	Hydrophilic surface fraction (MeOH)
Halo-C_{18}	0.150	0.146
Allure-C_{18}	0.114	0.094
Xterra-C_{18}	0.122	0.159
YMC-C_{18}	0.143	0.195
Gemini-C_{18}	0.122	0.210
Xbridge-C_{18}	0.117	0.165

Figure 3-35   Linearity of the adsorbed H_2O amount versus bonding density on
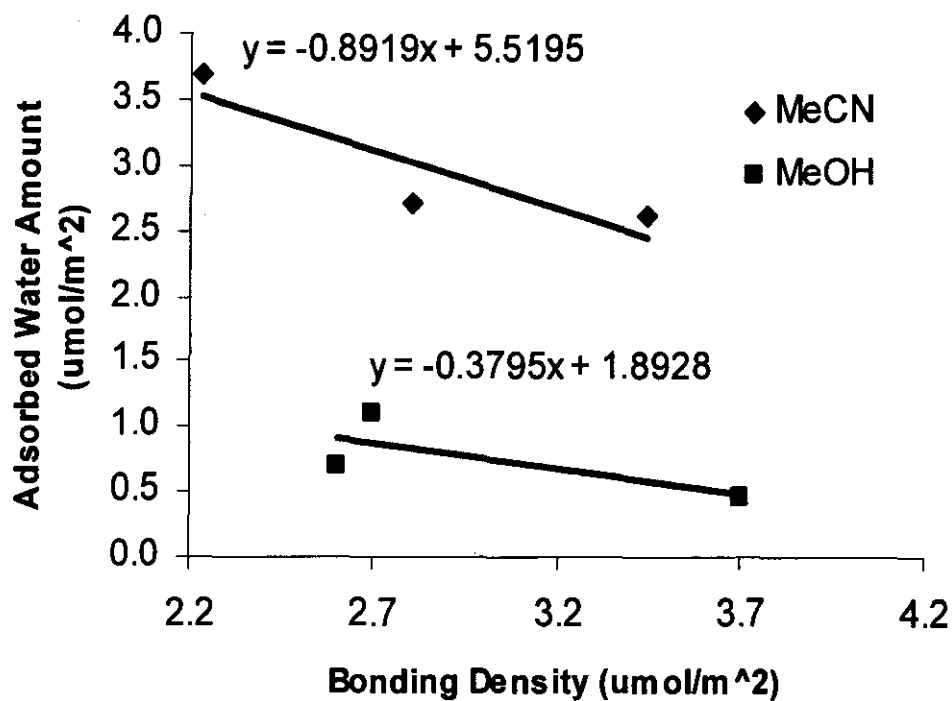
Halo-C_{18}, Allure-C_{18} and YMC-C_{18}

Table 3-15   Relationsip of adsorbed H₂O versus bonding density

Asorbent	Adorbed H_2O from MeCN (umol/m^2)	Adorbed H_2O from MeOH (umol/m^2)	bonding density (umol/m^2)
Halo-C_{18}	3.443	0.6855	2.6
Allure-C_{18}	2.232	0.4667	3.7
YMC-C_{18}	2.8	1.111	2.7

3.5   Conclusion

We demonstrated that surface-specific retention factors are more suitable for the comparison of chromatographic behavior of different reversed-phase columns under nearly ideal conditions, and in the absence of secondary equilibria effects. The calculation of surface-specific retention factors requires proper determination of the specific surface area of the packing material and the amount of packing material in the column. The specific surface area of chemically modified silica can be determined using standard LTNA measurements and by the application of BET theory. However, for C_{18}-type modified (hydrophobic) surfaces, the surface area values should be calculated using 20.5 Å^2 (instead of 16.2 Å^2) for the value of the nitrogen molecular area. The amount of adsorbent in the column can be determined from the difference between the column void volume and interparticle volume related to the specific pore volume of modified adsorbent. The everyday practical use of surface-specific retention factors could significantly simplify column selection and column comparison; although, for general chromatographers, these advantages will be realized only if column manufacturers regularly provide information about the adsorbent surface area and pore volume of the chemically modified surface.

The knowledge of the real surface area of the stationary phase is very important for the adsorption measurements. Calculation using a corrected surface of the stationary bonded phase is consistent with the theory and expectations. The interpretation of these isotherms had shown monomolecular character of MeOH adsorption and multi-player character of MeCN. On the modified silica surface, the effect of the residual silanols is not negligible, which is clearly demonstrated by the negative excess amounts of commonly used organic solvents. The H_2O mole fraction calculated from the adsorption isotherm gives clear evidence of the accessible residual silanols. It may be used to illustrate the heterogeneous character of the

surface of conventional chromatographic adsorbents, which is consistent with the simultaneous presence on their surface of residual silanols.

References:

1. U.D. Neue, B.A. Alden, T.H. Walrer, *J. Chromatogr., A* 1999, **849**, 101.

2. Y. Kazakevich, R. Lobrutto, HPLC for Pharmaceutical Scientists, 2007.

3. L. C. Snyder, J.J. Kirkland (Eds.), Introductin to Modern Liuqid Chromatography, Wiley-Interscience, New York, 1974.

4. F. Gritti, Guiochon, *J. Chromatogr., A* 2007, **1176**, 107-122.

5. T. Issaeva, A. Kourganov, K. Unger, *J. Chromatogr., A* 1999, **846**, 13-23

6. J. Kohler, P.D. Chase, R.D. Farlee, J. Vega, J.J. Kirkland, *J. Chromatogr.* 1986, **352**, 275.

7. J. Nawrocki, *J. Chromatogr., A* 1997, **779**, 29-71.

8. Bottoli CBG, Chaudry ZF, Fonseca DA, Collins KE, Collins CH, *J. Chromatogr., A* 2002, **948**, 121-128.

9. Tonhi E, Bachmann S, Albert K, Jardim ICSF, Collins CH, *J. Chromatogr., A* 2002, **948**, 97-107.

10. Jardim ICSF, Collins KE, Anazawa TA, *J. Chromatogr., A* 1999, **849**, 299-307.

11. G. Guiochon, *J. Chromatogr. A* 2007, **1168**, 101.

12. K. Cabrera, *J. Sep., Sci.* 2004, **27**, 843.

13. N. Ishizuka, H. Kobayashi, H. Minakuchi, K. Nakanishi, K. Hosoya, T. Ikegami, *J. Chromatogr., A* 2005, **960**, 85.

14. H. Zou, X. Huang, M. Ye, Q. Luo, *Jchromatogr., A* 2002, **954**, 5.

15. J.J. Kirkland, *J. Chromatogr., Sci.* 1969, 7, 7.

16. S. Brunauer, P.H.Emmet, E. Teller, *J. Am. Chem., Soc.* 1938, **60**, 309 – 319.

17. S.J. Gregg, K.S.W. Sing, Adsorption, Surface area and Porosity, Academic Press, London, 1976.

18. N.E. Buyanova, R.V. Zagrafskaya, A.P. Karnaukhov, A.S. Shepelina, *Kinetica i Cataliz*, 1983, **24**, 1011-1023.

19. J.L. Bass, B.W. Sands, P.W. Bratt, *Silanes, Surfaces and Interfaces.* ed. Leydel D.E., 1986, 1, 267-282.

20. S. Kiahara, K. Tanaka, T. Sakata, H. Muraishi, *J. Colloid Inferface Sci.* 1981, **84**, 519.

21. J.L. Bass, B.W. Sands, P.W. Bratt, in: *Proceedings of the Silanes, Surfaces, and Interfaces Symposium*, Snowmass, Co, June 1985, **267**, 19-21,.

22. I. Rustamov, T. Farcas, F. Ahmed, F. Chan, R. LoBrutto, H.M. McNair, Y.V. Kazakevich, *J. Chromatogr., A*, 2001, **913**, 49-63.

23. L.R. Snyder, J.J. Kirkland, and J.L. Glajch, *Practical HPLC Method Development*, 2nd ed., Jhn Wiley & Sons, New York, 1997.

24. Y. Bereznitski, M. Jaroniec, M.E. Gangoda, *J. Chromatogr., A* 1998, **828**, 59.

25. L.C. Sander, C.J. Glinka, S.W. Wise, Silanes, *Surfaces, and Interfaces, Proceedings*, Colorado, 1985, **431**.

26. F. Gritti, G. Guiochon, *J. Chromatogr., A*, 2005, **1099**, 1.

27. A. Vailaya, C. Horvath, *J. Chromatogr., A*, 1988, **829**, 1.

28. Y.V. Kazakevich, *J. Chromatogr., A*, 2006, **1126**, 232.

29. T.L. Chester, J.W. Coym, *J. Chromatogr., A*, 2003, **1003**, 101.

30. J.W. Gibbs, *On the equilibrium of heterogeneous substances. Collected Works*, Longmans, New York, 1928, pp. 55.

31. Cs. Horvath, W.R. Melander, I. Molnar, *J. Chromatogr.* 1976, **125**, 129.

32. L.C. Sander, S.A. Wise, *Anal. Chem.* 1984, **56**, 504.

33. K.B. Sentell, J.G. Dorsey, *J. Chromaotgr.* 1989, **461**, 193.

34. C. Cramers, A. Keulemans, H. McNair, in: E. Heftmann (Ed.), Chromatography, Reinhold, NY, 1961.

35. J.F.K. Huber, R.G. Gerritse, *J. Chromatogr.* 1971, **58**, 137-158.

36. F. Riedo, E. Sz. Kovats, *J. Chromatogr.* 1982, **239**, 1-28.

37. Y.A. Eltekov, Y.V. Kazakevich, *J. Chromatogr.* 1987, **395**, 473-480.

38. J. Zhu, A.M. Katti, G. Guiochon, *J. Chromatogr. A* 1991, **552**, 71-89.

39. G. Foti, C.D. Reyff, E.S. Kovats, *Langmuir* 1990, **6**, 759.

40. F. Koster, G.H. Findenegg, *Chromatographia* 1982, **15**, 743.

41. K. Miyabe, M. Suzuki, *AIChE J.* 1995, **41**, 536.

42. H. Poppe, *J. Chromatogr., A* 1993, **656**, 19-36.

43. F. Riedo and E. Kovats, *J. Chromatogr.* 1982, **239**, 1-28.

44. Y.V. Kazakevich, R. LoBrutto, F. Chan, T. PATEL, *J. Chromatogr., A* 2001, **913**, 75-87.

45. C.S. Koch, F. Koster, G.H. Findenegg, *J. Chromatogr.* 1987, **406**, 257-273.

46. S. Kitahara, K. Tankara, T. Sakata, H. Muraishi, *J. Colloid Interface Sci.* **84**, 519-525.

47. M. Jaroniec, *J. Chromatogr., A* 1993, **656**, 37

48. F. Gritti, G. Guiochon, *J. Chromatogr., A* 2007, **1155**, 85.

49. C. Horvath (Ed.), High Performance Liquid Chromatography, Advances and Perspectives, Academic Press, New York, 1980.

50. D.H. Everett, *J. Chem. Soc., Farady Trans* 1964, I **60**, $_1$803.

51. D.H. Everett, *Pure Appl. Chem.* 1981, **51**, 2$_1$81.

52. A.V. Kiselev, Z.F. *Khimii*, 1956, **25**, 705.

53. A.V. Kiselev, L.F. Pavlova, Physical Chemistry, pp $_1$8-27, January 1965.

54. R.M. McCormick, B. Karger, *Anal. Chem.* 1980, **52**, 2249-2255.

55. H.L. Wang, U. Duda, C.J. Radke, *J. Colloid Interf. Sci.* 1978, **66**, 152.

56. J. Jacobson, J. Frenz, Cs. Horvath, *J. Chromatogr.* 1984, **316**, 53.

57. Y.A. Eletov, Y. V. Kazakevich, A.V. Kiselev, A.A. Zhuchkov, *Chromaotraphia* 1985, **20**, 525.

58. J. Huang, C. Horvath, *J. Chromatogr.* 1987, **406**, 275.

59. J. Knox, R. Kaliszan, *J. Chromatogr.* 1985, **349**, 211.

60. K. Miyabe, M. Suzuki, *J. Chem. Eng. Jpn.* 1994, **27**, 785.

61. K. Miyabe, M. Suzuki, *AIChE J.* 1995, **41**, 536.

62. K. Miyabe, M. Suzuki, *AIChE J.* 1995, **41**, 548.

63. Y.A. Eltekov, Y.V. Kazakevich, *J. Chromatogr.* 1987, **395**, 473.

64. Y.V. Kazakevich, H.M. McNair, *J. Chromatogr., Sc.* 1995, **33**, 321.

65. G. Foty, M.L. Belvito, A. Alvarez-Zepeda, E. Kovats, *J. Chromatogr.* 1993, **630**, 1.

66. N.L. Ha, J. Ungvaral, E. Kovats, *Anal. Chem.* 1982, **54**, 2410.

67. D.H. Everett, J. Chem. Soc. Faraday Trans I, 1964, **60**, $_{18}$03-$_{18}$13.

68. B. Buszewski, M. Jezierska, M. Welniak, D. Berek, *J. High Resolut. Chromatogr.* 1998, **21**, 267

69. K. Krupczynska, P. Jandera, B. Buszewski, *Anal. Chem.* 2004, **76**, 227A.

70. R. Gadala-Kopciuch, B. Buszewski, *J. Sep. Sci.* 2003, **26**,1273.

71. J. Nawrocki, *J. Chromatogr., A* 1997, **779**, 29-71.

72. F. Gritti, G. Guiochon, *J. Chromatogr. A*, in press (JCA-C996).

73. F. Gritti, G. Guiochon, *Anal. Chem.* 2005, **77**, 1020.

74. U.D. Neue, D.J. Phillips, T.H. Walter, M. Capparella, B. Alden, R.P. Fisk, *LC-GC* 1994, **12** (6), 468.

75. D.V. McCalley, *Anal. Chem.* 2003, **75**, 3404.

76. F. Gritti, G. Guiochon, *J. Chromatogr., A* 2004, **1028**, 75.

77. F. Gritti, G. Guiochon, *Anal. Chem.* 2003, **75**, 5726.

78. F. Gritti, G. Guiochon, *J. Chromatogr., A* 2006, **1103**, 43-56.

79. F. Gritti, G. Guiochon, *J. Chromatogr., A* 2007, **1169**, 111-124.

80. F. Gritti, G. Guiochon, *J. Chromatogr., A* 2006, **1103**, 57-68.

81. F. Gritti, G. Guiochon, *J. Chromatogr., A* 2006, **1131**, 151-165.

82. F. Gritti, G. Guiochon, *J. Chromatogr., A* 2006, **1103**, 69-82.

83. N. Tanaka, H. Goodell, B. Karger, *J. Chromatogr.* 1978, **158**, 233.

84. M. Spanjer, C. De Ligny, *Chromatographia* 1985, **20**, 120.

85. R. Smith, *J. Chromatogr. A* 1993, **656**, 381.

86. T. Dzido, H. Englehardt, *Chromatographia* 1994, **39**, 51.

87. T. Dzido, *J. Liq. Chromatogr. & Rel. Tchnol.* 2000, **23**, 2773.

88. T. Dzido, T. Kossowski, D. Matosiuk, *J. Chromatogr., A* 2002, **947**, 167.

89. P. Zhuang, R. Thompson, and T. O'Brien, *Liq. Chromatogr. & Rel. Tchnol.* 2005, **23**, 1345-1356.

90. S. Cole, J. Dorsey, *J. Chromatogr.* 1993, **635**, 177.

91. O. Wan, R. Ramaley, *Chromatographia* 1998, **48**, 523.

92. J. Pemberton, M. Christopher, J. Orendorff, M. Ducey, *J. Chromatogr., A* 2001, **913**, 243.

93. R.P.W. Scott, P.J. Kucera, *J. Chromatogr.* 1977, **142**, 213.

94. R.P.W. Scott, P.J. Kucera, *J. Chromatogr.* 1979, **175**, 51.

95. D. Westerlund, A. Theodorsen, *J. Chromatogr.* 1977, **144**, 27.

96. D. Westerlund, A. Theodorsen, *J. Chromatogr.* 1980, **52**, 2249.

97. F. Gritti, G. Guiochon, *Anal. Chem.* 2005, 77, 4257-4272.

98. L. R. Synder, Principles of adsorption chromatography, Marcel Dekker, New York, 1968.

99. E. Soczewinski, M. Waksmundzka-Hajons, *J. Liq. Chromatogr.* 1980, 3, 1625-1636.

100. P.J. Schoenmakers, H.A.H. Billiet, R. Tijssen, L. de Galan, *J. Chromatogr.* 1978, **149**, 519-537.

101. P. Jandera, H. Colin, G. Guiochon, *Ana. Chem.* 1982, **54**, 435-441.

102.   L.R. Snyder, J.W. Dolan, J.R. Gant, *J. Chromatogr.* 1979, **165**, 3-30.

103.   P.W. Carr, J. Li, A.J. Dallas, D.I. Eikens, L.C. Tan, *J. Chromatogr., A* 1993, **656**, 113-133.

104.   B.L. Karger, J.R. Grant, A. Hartkopf, P.H. Weiner, *J. Chromatogr.* 1976, 128, 65-78.

105.   Cs. Horvats, W. Melander, Reversed-Phase Chromatography, in High Performance Liquid Chromatography Advances and Perspectives v. **2** Cs. Horvats ed. Academic Press 1980 NY pp 113-303.

106.   H. Colin, G. Guiochon, *J. Chromatogr.* 1977, **141** , 289-312.

107.   P.J.Schoenmakers, H.A. H. Billet, and L.de Galan, *J. Chromatogr.* 1979, **1985**, 179-195.

108.   U.D.Neue, C.HJ.Phoebe, K.Tran, Y. Cheng, Z.Lu, *J.Chromatogr., A* 2001, **925**, 49-67.

109.   P.Nikitas, A.Pappa-Louisi, *J. Chromatogr., A* 2001, **971**, 47-60.

110.   J.J. Kirkland, *J. Chromatogr., A* 2004, **1060**, 9–21.

111.   Uwe D. Neue, HPLC Columns, Wivey-VCH, 1997, New York, NY.

112.   Bocian, S.; Felinger, A.; Buszewski, B. Chromatographia online, Jan 2008.

113.   L.R. Snyder, J.J. Kirkland, J.L. Glajch, Practical HPLC Method Development, Wiley, 1997, NY , p 194.

114.   M. Jaroniec *J. of Chromatogr., A* 1993, **656**, 37-50.

115.   D. Visky , Y.V. Heyden , T. Ivanyi , P. Baten , J.D. Beer, Z. Kovacs , B. Noszal , P. Dehouck , E. Roets , Desire L. Massart , J. Hoogmartens, *J. Chromatogr., A* 2003, **1012**, 11-29

116.   R.J.M. Vervoort, A.J.J. Debets, H.A. Claessens, C.A. Cramers, G.J. de Jong, *J. Chromatrogr., A* 20008, **97**,1-22.

117.   H. A. Claessenes, M.A. van Straten, C.A. Cramers, M. Jezierska, B. Buszewski, *J. Chromatrogr., A* 1998, **826**, 135.

118.   waters Inc. http://www.waters.com

119.   Phenomenex Inc. http://www.phenomenex.com

120.   http://www.mac-mod.com/pb/halo-pb.html

121.   McElwee, J.; Helmy, R.; Fadeev, A. Y. *J. Colloids Interface Sci.* 2005, **285**, 551-556.

122.   Buszewski B, Krupczynska K, Gadzala-Kopiuch RM, Rychlicki G, Kaliszan R. *J. Sep. Sci.* 2003, **26**,313-321.

123.   Yamauchi H., Kondo S. *Colloid Polym Sci.* 1988, **266**, 855-861.